

Lehigh University Lehigh Preserve

Fritz Laboratory Reports

Civil and Environmental Engineering

1959

Buckling of uniformly compressed steel plates in the strain-hardening range, August 1956

G. Haaijer

Follow this and additional works at: <http://preserve.lehigh.edu/engr-civil-environmental-fritz-lab-reports>

Recommended Citation

Haaijer, G., "Buckling of uniformly compressed steel plates in the strain-hardening range, August 1956" (1959). *Fritz Laboratory Reports*. Paper 1423.

<http://preserve.lehigh.edu/engr-civil-environmental-fritz-lab-reports/1423>

This Technical Report is brought to you for free and open access by the Civil and Environmental Engineering at Lehigh Preserve. It has been accepted for inclusion in Fritz Laboratory Reports by an authorized administrator of Lehigh Preserve. For more information, please contact preserve@lehigh.edu.

Welded Continuous Frames and Their Components

Progress Report No. 20

BUCKLING OF UNIFORMLY COMPRESSED STEEL PLATES IN
THE STRAIN-HARDENING RANGE

by

Geerhard Haaijer

This work has been carried out as a part of an investigation sponsored jointly by the Welding Research Council and the Department of the Navy with funds furnished by the following:

American Institute of Steel Construction
American Iron and Steel Institute
Institute of Research, Lehigh University
Column Research Council (Advisory)
Office of Naval Research (Contract No. 39303)
Bureau of Ships
Bureau of Yards and Docks

Fritz Engineering Laboratory
Department of Civil Engineering
Lehigh University
Bethlehem, Pennsylvania

August, 1956

Fritz Laboratory Report No. 205E.7

620.6
L5R7f.
No. 205E.7

T A B L E O F C O N T E N T S

	Page
1. SYNOPSIS	1
2. INTRODUCTION	3
3. BUCKLING OF RECTANGULAR ORTHOTROPIC PLATES	6
3.1 General	6
3.2 Plates with One Free Edge	9
3.3 Plates Supported Along All Four Edges	11
4. INCREMENTAL STRESS-STRAIN RELATIONS	13
4.1 General	13
4.2 Loading Function $f = J_2$	14
5. INFLUENCE OF INITIAL IMPERFECTIONS	17
5.1 General	17
5.2 Simplified WF Column	18
5.3 Simplified Cruciform Section	19
6. STRESS-STRAIN RELATIONS FOR THE STRAIN-HARDENING RANGE OF STEEL	22
6.1 Results of Coupon Tests	22
6.2 The Tangent-Modulus in Shear	24
6.3 Bi-Axial Normal Stresses	25
7. COMPARISON WITH TEST RESULTS	32
7.1 Compression Tests on Angles	32
7.2 Tests on Wide-Flange Shapes	34
7.3 Summary	35
8. ACKNOWLEDGMENTS	37
9. REFERENCES	38
10. NOMENCLATURE	40
TABLES	44
FIGURES	

1. SYNOPSIS

The application of plastic design to continuous frames constructed of wide-flange shapes, imposes more severe limitations on the geometry of these shapes than conventional elastic design. In regions where yielding starts first, the flanges must be able to sustain strains considerably larger than the yield strain without the occurrence of local (plate) buckling.

With this practical application in mind, the problem of buckling of steel plates compressed beyond the yield strain is treated in the present paper. In the strain-hardening range the material is considered to be homogeneous. However, because of the yielding process the material cannot be expected to remain isotropic. Therefore, general expressions for the buckling strength are derived assuming the material to have become orthogonally anisotropic.

Orthogonal anisotropy in the case of plane stress is expressed mathematically by stress-strain relations involving five moduli. Numerical values of the moduli are estimated from the incremental theory of plasticity taking the second invariant of the deviatoric stress tensor as the loading function. The influence of initial imperfections is taken into account through proper adjustment of the values of the moduli. In selecting these values due consideration is given to the results of buckling tests.

In the yielding range the average strain in the direction of loading is between the strain at which yielding starts and the strain at the beginning of strain-hardening. For this case the material is considered to be partly elastic and partly strained up to the strain-hardening range.

Finally, theoretical estimates are compared with test results.

It is considered that the theory adequately describes the behavior.

2. INTRODUCTION

Presently used steel wide-flange shapes are proportioned such that no local buckling occurs within the elastic range. Consequently they can safely be used for structures in which the design is based upon theoretical first yield as the limiting condition (conventional design). However, design based upon ultimate strength (plastic design) imposes more severe requirements on the sections with regard to local buckling. The structure will reach its full ultimate load only if those parts where yielding starts first, can undergo sufficiently large deformations. For framed structures constructed of wide-flange shapes the flanges at the above mentioned locations must then be able to sustain strains considerably larger than the yield strain. Consequently the flanges should be proportioned such that local (plate) buckling does not occur under this condition.

In order to solve problems of plate buckling the relationships between the increments of stresses and strains due to the deflection of the plate out of its plane must be known. Within the elastic range the assumption that the material is isotropic and homogeneous leads to predictions which are in good agreement with test results⁽¹⁾. A satisfactory transition curve for the range from the elastic limit stress to the yield stress can easily be obtained by applying Bleich's semi-rational theory to an effective stress-strain curve⁽²⁾.

During the yielding process the material is heterogeneous. Yielding takes place in so-called slip bands and the strain jumps from its value at the elastic limit to that at the beginning of strain-hardening⁽³⁾. When all the material has been strained to the strain-hardening range the material again becomes homogeneous. In the

strain-hardening range, stress-strain relations of different theories of plasticity could be applied. Such theories can be divided into two groups: deformation or total stress-strain relations and incremental stress-strain relations.

Bijlaard⁽⁴⁾ was first to apply deformation stress-strain relations to the plate buckling problem. The theory was developed further by Ilyushin⁽⁵⁾ and modified by Stowell⁽⁶⁾. Incremental stress-strain relations were applied by Handelman and Prager⁽⁷⁾. An extensive survey of stress-strain relations in the plastic range has been made by Drucker⁽⁸⁾. Although the necessity for an incremental type of mathematical theory of plasticity has been shown, the results of plastic buckling tests on aluminum plates are well correlated by a deformation theory and bear no resemblance to predictions of incremental theory. Onat and Drucker⁽⁹⁾ investigated the influence of initial imperfections on torsional buckling for a simplified model of a cruciform section. For this case the paradox appears at its worst. Onat and Drucker showed that incremental plasticity leads to proper results when unavoidable initial imperfections are taken into account.

All theories of plate buckling in the plastic range imply orthotropic behavior of the material. This assumption seems to be very reasonable. Therefore, in the present report general expressions for the buckling strength of orthotropic plates are derived from general stress-strain relations involving five moduli (Chapter 3). Tests of steel tubes under combined compression and torsion showed that the behavior of the material is well described by the incremental theory

Generalities on stress and strain and incremental stress-strain relations are summarized in Chapter 4. The influence of initial imperfections is illustrated in Chapter 5. From the results of coupon tests numerical values of the moduli are then obtained in Chapter 6. The influence of initial imperfections is taken into account through adjustment of the values of the moduli. Combining the results of Chapters 3 and 6 gives numerical solutions of the plate buckling problem which are compared with test results in Chapter 7.

In summary, then, the objective is to predict the strain at which buckling occurs in steel plate elements when the strain has exceeded the elastic limit.

3. BUCKLING OF RECTANGULAR ORTHOTROPIC PLATES

3.1 General

Consider a rectangular steel plate taking the center plane of the plate as the x - y coordinate plane. Compressing the plate in the x - direction into the strain-hardening range may affect all deformation properties of the material. Hence the tangent moduli, E_x and E_y in the x - and y - direction respectively, are probably different. The same may hold for the coefficients of dilatation, ν_x and ν_y in the x - and y - direction. The shear modulus, G_t , may also be affected.

Thus

$$\left. \begin{aligned}
 \frac{\partial \epsilon_x}{\partial \sigma_x} &= \frac{1}{E_x} & \frac{\partial \epsilon_y}{\partial \sigma_y} &= \frac{1}{E_y} \\
 \frac{\partial \epsilon_x}{\partial \sigma_y} &= -\frac{\nu_y}{E_y} & \frac{\partial \epsilon_y}{\partial \sigma_x} &= -\frac{\nu_x}{E_x} \\
 \frac{\partial \gamma_{xy}}{\partial \tau_{xy}} &= \frac{1}{G_t}
 \end{aligned} \right\} \dots \dots (3.1)$$

where

- ϵ = normal strain
- γ = shear strain
- σ = normal stress
- τ = shear stress

Then the relations between the increments of strains and stresses can be written as follows:

$$\left. \begin{aligned} d\epsilon_x &= \frac{1}{E_x} d\sigma_x - \frac{\nu_y}{E_y} d\sigma_y \\ d\epsilon_y &= -\frac{\nu_x}{E_x} d\sigma_x + \frac{1}{E_y} d\sigma_y \\ d\gamma_{xy} &= \frac{1}{G_t} d\tau_{xy} \end{aligned} \right\} \dots \dots (3.2)$$

If equations (3.2) are valid for the entire cross-section the expressions for the bending and twisting moments in terms of the deflection, w , in the direction of the z -axis become

$$M_x = -\frac{E_x I}{1 - \nu_x \nu_y} \left[\frac{\partial^2 w}{\partial x^2} + \nu_y \frac{\partial^2 w}{\partial y^2} \right] \dots \dots (3.3)$$

$$M_y = -\frac{E_y I}{1 - \nu_x \nu_y} \left[\frac{\partial^2 w}{\partial y^2} + \nu_x \frac{\partial^2 w}{\partial x^2} \right] \dots \dots (3.4)$$

$$M_{xy} = -2 G_t I \frac{\partial^2 w}{\partial x \partial y} \dots \dots (3.5)$$

where

$$I = \frac{t^3}{12}$$

t = thickness of plate.

The condition that the bent position is in equilibrium can be expressed by the following differential equation:

$$D_x \frac{\partial^4 w}{\partial x^4} + 2H \frac{\partial^4 w}{\partial x^2 \partial y^2} + D_y \frac{\partial^4 w}{\partial y^4} = -\frac{t\sigma_x}{I} \frac{\partial^2 w}{\partial x^2} \dots \dots (3.6)$$

where

$$D_x = \frac{E_x}{1 - \nu_x \nu_y}$$

$$D_y = \frac{E_y}{1 - \nu_x \nu_y}$$

$$D_{xy} = \frac{\nu_y E_x}{1 - \nu_x \nu_y}$$

$$D_{yx} = \frac{\nu_x E_y}{1 - \nu_x \nu_y}$$

$$2H = D_{xy} + D_{yx} + 4G_t$$

The derivation of these equations may be found in the pertinent literature(11). Only if $H^2 = D_x D_y$, an assumption made by Bleich(2), can solutions of this differential equation be easily obtained.

If the plate is initially perfectly plane the value of σ_x at which bifurcation of equilibrium occurs (the plane and the bent position are both equilibrium positions) is determined by equation (3.6). The condition that both the plane and the bent position are equilibrium positions can also be expressed in terms of work. The additional work done by the external forces due to bending of the plate must equal the change in internal energy of the plate.

This yields the following integral equation

$$\begin{aligned} \frac{\sigma_x t}{I} \iint \left(\frac{\partial w}{\partial x} \right)^2 dx dy &= \iint \left[D_x \left(\frac{\partial^2 w}{\partial x^2} \right)^2 + \right. \\ &+ D_y \left(\frac{\partial^2 w}{\partial y^2} \right)^2 + (D_{xy} + D_{yx}) \left(\frac{\partial^2 w}{\partial x^2} \right) \cdot \left(\frac{\partial^2 w}{\partial y^2} \right) + \\ &\left. + 4G_t \left(\frac{\partial^2 w}{\partial x \partial y} \right)^2 \right] dx dy \dots \dots (3.7) \end{aligned}$$

When external restraints are provided to the plate the right-hand side of equation (3.7) has to be supplemented by additional terms expressing the work done by these restraints.

By assuming an appropriate deflection surface, equation (3.7) gives an approximate solution. The degree of approximation depends upon the correctness of the assumed deflection surface. In any case the result will be conservative.

3.2 Plates With One Free Edge

For a rectangular plate with the loaded edges $x = 0$ and $x = l$ hinged, edge $y = 0$ restrained against rotation and edge $y = b$ free (Fig. 1) the following deflection surface is assumed

$$w = \left[A \frac{y}{b} + B \left\{ \left(\frac{y}{b} \right)^2 + a_1 \left(\frac{y}{b} \right)^3 + a_2 \left(\frac{y}{b} \right)^4 \right\} \right] \sin \frac{\pi x}{l} \quad (3.8)$$

The ratio B/A depends upon the amount of restraint. In the case of elastic restraint, where γ = moment per unit length required for a unit rotation

$$\beta = \frac{B}{A} = \frac{\gamma b}{2D_y I} \quad \dots \quad (3.9)$$

Deflection surface (3.8) is similar to the one used by Lundquist and Stowell⁽¹²⁾. It can be shown⁽²⁰⁾ that better results are obtained with equation (3.8) if the following values for a_1 and a_2 are used

$$\text{For } 0 < \beta < 0.1 \quad a_1 = -0.7$$

$$a_2 = 0.2$$

$$\text{and for } \beta = \infty \quad a_1 = -1.10$$

$$a_2 = 0.54$$

Substituting w in equation (3.7) and integrating gives

$$\begin{aligned} \sigma_x = & \frac{t^2}{12b^2} \left[D_x \left(\frac{\pi b}{l} \right)^2 + D_y \left(\frac{l}{\pi b} \right)^2 \frac{2\beta + \beta^2 C_3}{\frac{1}{3} + \beta C_1 + \beta^2 C_2} + \right. \\ & - (D_{xy} + D_{yx}) \cdot \frac{\beta C_4 + \beta^2 C_5}{\frac{1}{3} + \beta C_1 + \beta^2 C_2} + \\ & \left. + 4G_t \cdot \frac{1 + \beta C_6 + \beta^2 C_7}{\frac{1}{3} + \beta C_1 + \beta^2 C_2} \right] \quad \dots \quad (3.10) \end{aligned}$$

where

$$\begin{aligned} C_1 &= 1/2 + 2/5 a_1 + 1/3 a_2 \\ C_2 &= 1/5 + 1/3 a_1 + 1/7 (a_1^2 + 2a_2) + 1/4 a_1 a_2 + 1/9 a_2^2 \\ C_3 &= 4 + 12a_1^2 + 144/5 a_2^2 + 12a_1 + 16a_2 + 36a_1 a_2 \\ C_4 &= 1 + 2a_1 + 3a_2 \\ C_5 &= 2/3 + 2a_1 + 1/5 (6a_1^2 + 14a_2) + 3a_1 a_2 + 12/7 a_2^2 \\ C_6 &= 2 (1 + a_1 + a_2) \\ C_7 &= 4/3 + 3a_1 + 1/5 (9a_1^2 + 16a_2) + 4a_1 a_2 + 16/7 a_2^2 \end{aligned}$$

The minimum value, σ_{cr} , of σ_x is obtained for l/b given by

$$\frac{l}{b} = \pi \sqrt{\frac{\frac{1}{3} + \beta C_1 + \beta^2 C_2}{2\beta + \beta^2 C_3}} \cdot \sqrt{\frac{D_x}{D_y}} \quad \dots \quad (3.11)$$

In the limiting cases when the edge $y = 0$ is hinged or completely fixed equation (3.10) reduces to

a.) Edge $y = 0$ hinged ($\beta = 0$) and $l = L$

$$\sigma_{cr} = \left(\frac{t}{b} \right)^2 \left[\frac{\pi D_x}{12} \left(\frac{b}{L} \right)^2 + G_t \right] \quad \dots \quad (3.12)$$

For a long plate the first term can be neglected and

$$\sigma_{cr} = \left(\frac{t}{b} \right)^2 G_t \quad \dots \quad (3.13)$$

b.) Edge $y = 0$ completely fixed ($\beta = \infty$)

The minimum value, σ_{cr} , of σ_x is obtained when the half-wave length l satisfies

$$\frac{l}{b} = 1.46 \sqrt[4]{\frac{D_x}{D_y}} \quad \dots \quad (3.14)$$

Then

$$\sigma_{cr} = \left(\frac{t}{b}\right)^2 \left[0.769 \sqrt{D_x D_y} - 0.270 (D_{xy} + D_{yx}) + 1.712 G_t \right] \quad \dots \quad (3.15)$$

3.3 Plates Supported Along All Four Edges

The loaded edges $x = 0$ and $x = l$ are hinged and the edges $y = \pm d/2$ have equal restraint against rotation (Fig. 2). For this case the following deflection surface is used⁽¹³⁾

$$w = \left[B \pi \left(\frac{y}{d} - \frac{1}{4} \right) + (A+B) \cdot \cos \frac{\pi y}{d} \right] \sin \frac{\pi x}{l} \quad \dots \quad (3.16)$$

The ratio B/A depends on the amount of restraint. For elastic restraints with ψ = moment per unit length required for unit rotation

$$\beta = \frac{B}{A} = \frac{\psi d}{2 D_y I} \quad \dots \quad (3.17)$$

Substituting w from equation (3.16) in equation (3.7) and integrating gives

$$\begin{aligned} \sigma_x = & \frac{\pi^2 t^2}{12 d^2} \left[D_x \left(\frac{d}{l} \right)^2 + D_y \left(\frac{l}{d} \right)^2 \frac{\frac{1}{4} + (c_1 + \frac{2}{\pi^2}) \beta + \beta^2 c_3}{\frac{1}{4} + \beta c_1 + \beta^2 c_2} + \right. \\ & + (D_{xy} + D_{yx}) \frac{\frac{1}{4} + \beta c_1 + \beta^2 c_4}{\frac{1}{4} + \beta c_1 + \beta^2 c_2} + \\ & \left. + 4 G_t \cdot \frac{\frac{1}{4} + \beta c_1 + \beta^2 c_4}{\frac{1}{4} + \beta c_1 + \beta^2 c_2} \right] \quad \dots \quad (3.18) \end{aligned}$$

with

$$\begin{aligned} c_1 &= 0.09472 \\ c_2 &= 0.00921 \\ c_3 &= 0.04736 \\ c_4 &= 0.01139 \end{aligned}$$

The minimum value of σ_x is obtained for l given by

$$\frac{l}{d} = \sqrt[4]{\frac{D_x}{D_y} \frac{\frac{1}{4} + \beta c_1 + \beta c_2}{\frac{1}{4} + (c_1 + \frac{2}{\pi^2})\beta + \beta^2 c_3}} \quad \dots \quad (3.19)$$

In the limiting cases, when the unloaded edges $y = \pm d/2$ are hinged or completely fixed, the minimum values of σ_x are

a.) Edges $y = \pm d/2$ hinged ($\beta = 0$)

$$\sigma_{cr} = \frac{\pi^2}{12} \left(\frac{t}{d}\right)^2 \left[2\sqrt{D_x D_y} + D_{xy} + D_{yx} + 4G_t \right] \quad \dots \quad (3.20)$$

where

$$\frac{l}{d} = \sqrt[4]{\frac{D_x}{D_y}} \quad \dots \quad (3.21)$$

b.) Edges $y = \pm d/2$ completely fixed ($\beta = \infty$)

$$\begin{aligned} \sigma_{cr} = \frac{\pi^2}{12} \left(\frac{t}{d}\right)^2 \left[4.554\sqrt{D_x D_y} + 1.237(D_{xy} + D_{yx}) + \right. \\ \left. + 4.943 G_t \right] \quad \dots \quad (3.22) \end{aligned}$$

where

$$\frac{l}{d} = 0.664 \sqrt[4]{\frac{D_x}{D_y}} \quad \dots \quad (3.23)$$

In the following chapters values of D_x , D_y , D_{xy} , D_{yx} and G_t will be determined. On substituting these values in the above general expressions, numerical solutions to the local buckling problem will be obtained.

4. INCREMENTAL STRESS -
STRAIN RELATIONS

4.1 General

It is commonly assumed that yielding occurs whenever some function of stress, $f(\sigma_{ij})^*$, equals some number, k . If the material is originally isotropic this yield condition is independent of the orientation of the coordinate system. In this instance f must be a function of the stress invariants. An extension of the yield function is obtained by assuming the existence of a loading function, $f(\sigma_{ij})$, which depends upon the state of stress and strain and the history of loading. For ideally plastic materials plastic flow occurs whenever f equals some number k . For materials exhibiting strain-hardening plastic deformations occur when the loading function exceeds k .

Prager⁽¹⁵⁾ proved that, if

1. a loading function exists, and
2. the relation between infinitessimals of stress and strain is linear,

the only permissible stress-strain relation for strain-hardening material when loading is

$$d\epsilon_{ij}^p = F \frac{\partial f}{\partial \sigma_{ij}} \frac{\partial f}{\partial \sigma_{kl}} d\sigma_{kl} \quad \dots \quad (4.1)$$

* Tensor notation is used in referring to generalized stress and strain. Cartesian coordinates x_1 , x_2 , and x_3 , corresponding to the x , y , and z axis of engineering notation are denoted by letter subscripts i , j , k , l , which take the values 1, 2, and 3. Thus the nine components of stress and strain tensors are represented by single symbols σ_{ij} and ϵ_{ij} respectively. Repeated subscripts indicate summation. See e.g. Ref. 14.

and when unloading is

$$d\epsilon_{ij}^P = 0 \quad \dots \quad (4.2)$$

where ϵ_{ij}^P = plastic component of strain ϵ_{ij} and F and f are functions of stress and strain. The geometric proof of Prager's stress-strain law (equations 4.1 and 4.2) is also included by Drucker in his survey of stress-strain relations in the plastic range⁽⁸⁾.

As no information was available concerning the actual behavior of steel in the strain-hardening range a few tests were carried out on combined compression and torsion of steel tubes⁽¹⁰⁾. The tubes were compressed into the strain-hardening range and then subjected to torsion while keeping the axial load constant. It was found that for this particular loading path the behavior is very well described by Prager's incremental stress-strain relations taking $f = J_2$, where J_2 is the second invariant of the deviatoric stress tensor.*

Although these tests are by no means a general verification of this theory they give some indication of its possible validity. In view of these results and on account of its simplicity, the loading function $f = J_2$ will be applied in the following derivations.

4.2 Loading Function $f = J_2$

Applying the loading function $f = J_2$ to equations (4.1) and (4.2) gives

$$d\epsilon_{ij}^P = F s_{ij} dJ_2 \quad \dots \quad (4.3)$$

* The state of stress, with components σ_{ij} , can be split into two parts: a uniform tension (or compression), s , and another state of stress, with components s_{ij} , having the same shear stress but zero mean normal stress. The latter is called the deviatoric stress tensor. Thus $\sigma_{ij} = s_{ij} + s\delta_{ij}$ with $s = 1/3 \sigma_{ii}$. The second invariant is given by $J_2 = 1/2 s_{ij} s_{ij}$.

when $dJ_2 > 0$

and

$$d\epsilon_{ij}^p = 0 \quad \dots \quad (4.4)$$

when $dJ_2 \leq 0$

The increments of the elastic components, ϵ_{ij}^e , of the strains are given by Hooke's law

$$d\epsilon_{ij}^e = \frac{1+\nu}{E} d\sigma_{ij} - \frac{\nu}{E} d\sigma_{kk} \delta_{ij} \quad \dots \quad (4.5)$$

where

E = modulus of elasticity

ν = Poisson's ratio

δ_{ij} = Kronecker delta, defined as unity for $i = j$ and zero
for $i \neq j$

For the case of plane stress ($\sigma_z = \tau_{xz} = \tau_{yz} = 0$) the stress-strain relations, written in unabridged form, are

$$d\epsilon_x = \frac{1}{E} d\sigma_x - \frac{\nu}{E} d\sigma_y + \frac{1}{3} F (2\sigma_x - \sigma_y) dJ_2 \quad \dots \quad (4.6)$$

$$d\epsilon_y = -\frac{\nu}{E} d\sigma_x + \frac{1}{E} d\sigma_y + \frac{1}{3} F (2\sigma_y - \sigma_x) dJ_2 \quad \dots \quad (4.7)$$

$$d\epsilon_z = -\frac{\nu}{E} (d\sigma_x + d\sigma_y) - \frac{1}{3} F (\sigma_x + \sigma_y) dJ_2 \quad \dots \quad (4.8)$$

$$d\gamma = \frac{2(1+\nu)}{E} d\tau + 2F\tau dJ_2 \quad \dots \quad (4.9)$$

when

$$dJ_2 = \frac{1}{3} (2\sigma_x - \sigma_y) d\sigma_x + \frac{1}{3} (2\sigma_y - \sigma_x) d\sigma_y + 2\tau d\tau > 0 \quad \dots \quad (4.10)$$

and

$$d\epsilon_x = \frac{1}{E} d\sigma_x - \frac{\nu}{E} d\sigma_y \quad \dots \quad (4.11)$$

$$d\epsilon_y = -\frac{\nu}{E} d\sigma_x + \frac{1}{E} d\sigma_y \quad \dots \quad (4.12)$$

$$d\epsilon_z = -\frac{\nu}{E} (d\sigma_x + d\sigma_y) \quad \dots \quad (4.13)$$

$$d\gamma = \frac{2(1+\nu)}{E} d\tau \quad \dots \quad (4.14)$$

when

$$dJ_2 \leq 0$$

The function F can be obtained from the results of a simple coupon test for which $\sigma_y = \tau = d\sigma_y = d\tau = 0$

Denoting

$$\frac{d\sigma_x}{d\epsilon_x} = E_t \quad \dots \quad (4.15)$$

F is defined by equation (4.6) as

$$F = \frac{3}{4J_2} \left[\frac{1}{E_t} - \frac{1}{E} \right] \quad \dots \quad (4.16)$$

Because of unavoidable initial imperfections the above derived stress-strain relations cannot be applied without modification to the local buckling problem. After investigating the influence of initial imperfections on two simplified models in the next chapter effective stress-strain relations for the strain hardening range of steel will be derived in Chapter 6.

5. INFLUENCE OF INITIAL IMPERFECTIONS

5.1 General

A perfectly plane plate will remain plane if it is subjected to loads acting in its center plane which do not exceed the corresponding buckling loads. In the case of longitudinal loading in the x direction producing a state of stress with σ_x as the only component, this state of stress will remain unchanged up to the point when buckling occurs. Consequently the buckling stress can be obtained from stress-strain relations (4.6) to (4.9) with $\sigma_y = \tau = 0$.

However, the buckling strength of actual plates with unavoidable imperfections does not agree with the predictions for perfectly plane plates. The main reason for the discrepancy seems to be equation (4.9) which predicts elastic behavior with regard to the superimposed shear stresses.

Applying a simplified stress-strain diagram to a simplified model of a cruciform section Onat and Drucker⁽⁹⁾ have shown that small unavoidable imperfections may account for the difference between predicted and actual behavior. Apparently the influence of imperfections on sections which fail by torsional buckling is completely different from those which fail in bending. The latter case has been investigated by Wilder, Brooks and Mathauser⁽¹⁶⁾.

In the following, this difference in behavior will be illustrated for simplified models which buckle in the strain-hardening range. The applied simplified stress-strain curve with $n = E/E_t = 40$ is shown in Fig. 3. Reasons why the compressive stresses can exceed the yield stress, σ_0 , will be discussed in Chapter 6.

5.2 Simplified WF Column

The simplified WF column consists of two thin flanges of equal area separated by a web of infinite shear stiffness and negligible area (Fig. 4). Instead of a true initial imperfection, the deflections at the beginning of strain-hardening ($\sigma = \sigma_0$ and $\epsilon = \epsilon_0$) are used in the computations.

Following the same approach as Wilder, Brooks and Mathauser the deflection curve is assumed to be

$$y = \bar{y} \sin \frac{\pi x}{l} \quad \dots \quad (5.1)$$

At the beginning of strain-hardening

$$y_0 = \bar{y}_0 \sin \frac{\pi x}{l} \quad \dots \quad (5.2)$$

The load vs deflection curve is found by considering equilibrium of the center section of the column.

For the first part of the load vs deflection curve the strain in both flanges increases and the relation between average stress and deflection is given by

$$\frac{\sigma}{\sigma_0} = \frac{\sigma_t}{\sigma_0} - \left(\frac{\sigma_t}{\sigma_0} - 1 \right) \frac{f_0}{f} \quad \dots \quad (5.3)$$

where

σ = average stress of both flanges

$\sigma_t = \frac{\pi^2 E_t}{(l/r)^2}$ (tangent modulus stress)

$f = \bar{y}/d$

$d =$ depth of section

$f_0 =$ value of f at beginning of strain-hardening.

Strain reversal occurs for

$$f = f_s = \sqrt{\frac{1}{2} \left(1 - \frac{\sigma_e}{\sigma_t}\right)} f_0 \quad \dots \quad (5.4)$$

The corresponding stress, σ_s , is obtained from equation (5.3) by substituting $f = f_s$.

After strain-reversal has started the load vs deflection relation is given by

$$\frac{\sigma}{\sigma_0} \left[\frac{n-1}{2(n+1)} + f \right] = \frac{\sigma_s}{\sigma_0} \left[\frac{n-1}{2(n+1)} + f_s \right] + \frac{\sigma_t}{\sigma_0} \frac{2n}{n+1} (f - f_s) \quad \dots \quad (5.5)$$

Figure 6 shows curves of σ/σ_0 vs f for $\sigma_t/\sigma_0 = 1.2$ and different values of f_0 . The figure illustrates the behavior of the column for loads corresponding to stresses $\sigma \approx \sigma_t$. Although the deflections start to increase more rapidly the load continues to increase. Therefore it is safe to use the tangent modulus load, which corresponds to $\sigma = \sigma_t$, as the limit of usefulness of the column.

5.3 Simplified Cruciform Section

In contrast to the above example the influence of initial imperfections on the buckling strength of a column of simplified cruciform cross-section will now be illustrated. The solution of the problem as given by Onat and Drucker⁽⁹⁾ can be applied without modification to the simplified stress strain curve of Fig. 3.

The cross-section consists of a thin shell of constant thickness h (Fig. 5). The column which is loaded uniformly is assumed to fail by twisting. The ends are considered as providing no restraint, which

considerably simplifies the kinematics of the problem and makes the state of stress and strain the same at each cross-section. An approximate solution for small values of ψ is given as

$$\sigma = \frac{\sigma_0 \left(\frac{\psi_0}{\psi}\right)^{\frac{1}{2n'}} + \sigma_e \left[1 - \left(\frac{\psi_0}{\psi}\right)^{\frac{1}{2n'}}\right]}{1 + \frac{(n'-1)}{2n} (\psi - \psi_0)} \quad \dots \quad (5.6)$$

where

$$\psi = \frac{b^4}{3t^2} \theta^2$$

θ = angle of twist per unit length

$$n' = \frac{3G}{E_t} + 1 - \frac{3G}{E}$$

$$\sigma_e = \frac{3t^2}{b^2} G \quad (\text{elastic torsional buckling stress})$$

Results for the strain-hardening range of steel, $n' = 46$ ($n = 40$) are shown in Fig. 7. Load vs twist curves are plotted for initial imperfections $b\theta_0 = 0, 0.01^\circ$ and 0.1° , $b\theta$ being the angle of twist between two cross-sections a distance b apart. In all cases the ratio of the elastic buckling stress to the yield stress is five.

$$(\sigma_e/\sigma_0 = 5)$$

It is seen that very small imperfections cause a considerable reduction of the column strength. A perfectly straight member would reach its elastic buckling load, for the case considered $\sigma_e/\sigma_0 = 5$. An imperfection at $\sigma = \sigma_0$ and $\epsilon = \epsilon_0$ of $b\theta_0 = 0.01^\circ$ reduces the maximum load to $\sigma_m/\sigma_0 = 1.4$. Consequently the application of the J_2 incremental theory to a perfectly plane plate which fails primarily by twisting cannot be expected to correctly predict the buckling strength of actual plates.

Rather than attempt to solve the buckling problem of a plate with initial imperfections, effective stress-strain relations are determined in the next chapter. It will be necessary to modify the values of D_x , D_y , D_{xy} , D_{yx} , and G_t such that the application to the general expressions of Chapter 3 will result in a correct description of the behavior of actual plates.

6. STRESS - STRAIN RELATIONS
FOR THE STRAIN - HARDENING
RANGE OF STEEL

6.1 Results of Coupon Tests

A simplified stress-strain curve obtained from a simple coupon test is shown in Fig. 3. It must be borne in mind that the strain represents an average strain measured over a certain gage length. It would be entirely erroneous to assume that the local strains within the plastic range from ϵ_f to ϵ_0 are equal to the average strain. Yielding of mild steel occurs in small slip bands⁽³⁾. Slip takes place in a "jump" such that the strain across such a narrow band jumps from ϵ_f to ϵ_0 . The first slip band originates at a weak point in the specimen, due to an inclusion, a stress concentration or other defects. From there on yielding will spread along the specimen.

This consideration leads to the conclusion that there is no material within the specimen at a strain between the yield strain, ϵ_f , and the strain-hardening strain, ϵ_0 . Either the material is still elastic or it has reached the strain-hardening range.

In the strain-hardening range, $\epsilon > \epsilon_0$, the material is again homogeneous and in this range the "J₂ theory of plasticity" will be applied. In the intermediate range, $\epsilon_f < \epsilon < \epsilon_0$, the specimen can be considered to consist of two materials.

The results of 21 compression coupon tests carried out at Fritz Engineering Laboratory are summarized in Table 1. The coupons were cut from the flanges of WF shapes and from angles. For the interpretation of the results of coupon tests the following must be taken into account.

Coupons are tested continuously in a hydraulic testing machine. It has become customary in Fritz Laboratory to test coupons with a valve opening of the machine corresponding to a strain rate of 1 micro in./in. per second in the elastic range. It has been shown by Huber and Beedle⁽¹⁷⁾ that the ratio of the yield stress of a static test (where the load settles down after each increment of strain) and the yield stress of a continuous coupon test is approximately 0.925. Consequently a value of the yield stress, σ_0 , of $0.925 \times 39.2 = 36$ ksi will be used in the following derivations.

Stress-strain curves for the strain-hardening range as obtained from 5 selected coupon tests have been replotted in Fig. 8. Coupons 9 and 18 represent the extreme cases while 5, 15, and 17 represent tests with "average" results.

The average stress-strain curve for the strain-hardening range can be expressed by the three parameters introduced by Ramberg and Osgood⁽¹⁸⁾.

$$\epsilon - \epsilon_0 = \frac{\sigma - \sigma_0}{E_0} + K \left(\frac{\sigma - \sigma_0}{E_0} \right)^m \quad \dots \quad (6.1)$$

where

$$\begin{aligned} \sigma_0 &= 36 \text{ ksi} \\ \epsilon_0 &= 14 \times 10^{-3} \text{ in./in.} \\ E_0 &= 900 \text{ ksi}^* \\ K &= 21 \\ m &= 2 \end{aligned}$$

Equation (6.1) is also plotted in Fig. 8.

* The values of E_0 in Table 1 are taken from Fritz Laboratory reports in which they are usually not given as the slope of the stress-strain curve at the initiation of strain-hardening but as the slope at a strain somewhat larger than ϵ_0 . Consequently E_0 as used in equation (6.1) is larger than the average value given in Table 1.

The information now available is sufficient to determine F (J_2) defined by equation (4.16). From equations (4.16) and (6.1) it follows that

$$F = \left[67.357 \frac{1}{\sqrt{J_2}} - 591.667 \frac{1}{J_2} \right] \times 10^{-6} \frac{\text{in}^6}{\text{kips}^3} \dots \dots (6.2)$$

for $J_2 > 1/3 \sigma_0^2 = 432 \text{ kips}^2/\text{in.}^4$

6.2 The Tangent-Modulus In Shear

Consider the case where shear stresses, τ , are superimposed on a constant normal stress, σ_x , taking $\sigma_y = 0$ and $d\sigma_x = d\sigma_y = 0$. The relations between the increments of stress and strain given by equations (4.6) and (4.9) reduce to

$$d\epsilon_x = \frac{4}{3} F \sigma_x \tau d\tau \dots \dots (6.3)$$

$$d\gamma = \frac{2(1+\nu)}{E} d\tau + 4F\tau^2 d\tau \dots \dots (6.4)$$

Integrating equation (6.4) gives the relationship between τ and γ as shown in Fig. 9 for $\sigma_x = 36 \text{ ksi}$ and $\sigma_x = 48 \text{ ksi}$. The corresponding slope

$$G_t = \frac{d\tau}{d\gamma} \dots \dots (6.5)$$

is plotted in Fig. 10.

It is seen from Fig. 10 that the value of G_t drops rapidly for small values of γ . However, in the region $2,000 \text{ ksi} < G_t < 3,000 \text{ ksi}$ the decrease becomes slower. Consequently any value in this region

could be selected as a useful value of G_t for the strain-hardening range of steel. On account of the results of torsional buckling tests on angle specimens presented in Chapter 7, the value $G_t = 2,400$ ksi is selected as being applicable to the strain-hardening range. From Fig. 9 it follows that the influence of the magnitude of the normal stress can be neglected for that part of the strain-hardening range under consideration.

6.3 Bi-Axial Normal Stresses

For regions of a plate in which cross bending is of importance the shear stresses are zero or very small, e.g. the center of plates supported along all four edges or the fixed edge of a clamped outstanding flange.

In this case equations (4.6) and (4.7) reduce to

$$d\epsilon_x = \left[\frac{1}{E} + \frac{1}{9} F (2\sigma_x - \sigma_y)^2 \right] d\sigma_x + \\ - \left[\frac{\nu}{E} - \frac{1}{9} F (2\sigma_x - \sigma_y)(2\sigma_y - \sigma_x) \right] d\sigma_y \quad \dots \quad (6.6)$$

$$d\epsilon_y = \left[\frac{1}{E} + \frac{1}{9} F (2\sigma_y - \sigma_x)^2 \right] d\sigma_y + \\ - \left[\frac{\nu}{E} - \frac{1}{9} F (2\sigma_x - \sigma_y)(2\sigma_y - \sigma_x) \right] d\sigma_x \quad \dots \quad (6.7)$$

Comparing equations (6.6) and (6.7) with equations (3.2) gives

$$\frac{1}{E_x} = \frac{1}{E} + \frac{1}{9} F (2\sigma_x - \sigma_y)^2 \quad \dots \quad (6.8)$$

$$\frac{1}{E_y} = \frac{1}{E} + \frac{1}{9} F (2\sigma_y - \sigma_x)^2 \quad \dots \quad (6.9)$$

$$\nu_x = \frac{\frac{\nu}{E} - \frac{1}{9} F (2\sigma_x - \sigma_y)(2\sigma_y - \sigma_x)}{\frac{1}{E} + \frac{1}{9} F (2\sigma_x - \sigma_y)^2} \dots \dots (6.10)$$

$$\nu_y = \frac{\frac{\nu}{E} - \frac{1}{9} F (2\sigma_x - \sigma_y)(2\sigma_y - \sigma_x)}{\frac{1}{E} + \frac{1}{9} F (2\sigma_y - \sigma_x)^2} \dots \dots (6.11)$$

For a perfectly plane plate ($\sigma_y = 0$) equations (6.8) to (6.11)

reduce to

$$E_x = E_t \dots \dots (6.12)$$

$$E_y = \frac{4E E_t}{E + 3E_t} \dots \dots (6.13)$$

$$\nu_x = \frac{E - (1 - 2\nu) E_t}{2E} \dots \dots (6.14)$$

$$\nu_y = \frac{2E - (1 - 2\nu) E_t}{E + 3E_t} \dots \dots (6.15)$$

Equations (6.12) to (6.15) have been applied with different notation by Handelman and Prager(7).

Equations (6.9) to (6.11) are valid only if

$$dJ_2 > 0 \dots \dots (6.16)$$

or rewritten

$$2d\sigma_x - d\sigma_y > 0 \dots \dots (6.17)$$

and with equations (6.6) and (6.7)

$$(2 - \nu) de_x - (1 - 2\nu) de_y > 0 \dots \dots (6.18)$$

Figure 11 shows the assumed linear strain distribution due to curvatures dK_x and dK_y in the x - and y - directions.

$$d\epsilon_x = d\epsilon_1 + z dK_x \quad \dots \quad (6.19)$$

$$d\epsilon_y = d\epsilon_2 + z dK_y \quad \dots \quad (6.20)$$

where $d\epsilon_1$ and $d\epsilon_2$ are strain increments of the central plane in the x- and y-direction and z is the distance to the central plane.

The condition that all of the section is deformed plastically is obtained by substituting equations (6.19) and (6.20) in equation (6.18)

$$(2-\nu)(d\epsilon_1 + z dK_x) - (1-2\nu)(d\epsilon_2 + z dK_y) > 0 \quad (6.21)$$

$$\text{for } -t/2 \leq z \leq t/2$$

The increase of the force per unit width in the x - direction, N_x , is found by rearranging equation (3.2) and integrating over the thickness of the plate

$$\begin{aligned} dN_x &= \int_{-t/2}^{t/2} (d\sigma_x) dz = \\ &= D_x t (d\epsilon_1 + \nu_y d\epsilon_2) \end{aligned} \quad \dots \quad (6.22)$$

The increase of the force per unit width in the y - direction is

$$\begin{aligned} dN_y &= \int_{-t/2}^{t/2} (d\sigma_y) dz = \\ &= D_y t (d\epsilon_2 + \nu_x d\epsilon_1) \end{aligned} \quad \dots \quad (6.23)$$

However, no external forces are applied in the y - direction, thus

$$dN_y = 0 \quad \dots \quad (6.24)$$

or

$$d\epsilon_2 = -\nu_x d\epsilon_1 \quad \dots \quad (6.25)$$

Substituting equation (6.25) in (6.22) gives

$$dN_x = E_x t d\epsilon_1 \quad \dots \quad (6.26)$$

The plasticity condition, equation (6.21), then becomes

$$\left[2-\nu+(1-2\nu)\nu_x\right]d\epsilon_1+(2-\nu)zdk_x-(1-2\nu)zdk_y > 0 \quad \dots \quad (6.27)$$

for $-t/2 \leq z \leq t/2$

If the neutral zone between loading and unloading zones is at $z = t/2$, equation (6.27) gives

$$d\epsilon_1 = \frac{t/2\{(2-\nu)dk_x - (1-2\nu)dk_y\}}{2-\nu+(1-2\nu)\nu_x} \quad \dots \quad (6.28)$$

Obviously $d\epsilon_1 > 0$ only if

$$dk_y < \frac{2-\nu}{1-2\nu} dk_x \quad \dots \quad (6.29)$$

Checking the plasticity condition (6.27) for $d\epsilon_1$ given by equation (6.21) shows that condition (6.27) is not violated if (6.29) is satisfied.

If the neutral zone is at $z = -t/2$ equation (6.27) gives

$$d\epsilon_1 = \frac{t/2[(1-2\nu)dk_y - (2-\nu)dk_x]}{2-\nu + (1-2\nu)\nu_x} \dots \dots (6.30)$$

and $d\epsilon_1 > 0$ only if

$$dk_y > \frac{2-\nu}{1-2\nu} dk_x \dots \dots (6.31)$$

The plasticity condition (6.27) is not violated if equation (6.31) is satisfied.

From equations (6.28) and (6.30) it is seen that

$$d\epsilon_1 = 0$$

and consequently according to equation (6.26)

$$dN_x = 0$$

for

$$dk_y = \frac{2-\nu}{1-2\nu} dk_x \dots \dots (6.32)$$

Furthermore $dJ_2 = 0$ for the entire cross-section. Thus

$$d\sigma_x = \frac{1}{2} d\sigma_y \dots \dots (6.33)$$

for an initially plane plate with $\sigma_y = 0$.

In this case, since bending is not accompanied by an increase in axial load the influence of initial imperfections will be the greatest.

Suppose biaxial loading starts at $\sigma_x = \sigma_x^*$, $\sigma_y = 0$, $\epsilon_x = \epsilon_x^*$, $\epsilon_y = \epsilon_y^*$. Then it follows from equation (4.10) with equation (6.33) that initially

$$dJ_2 = \frac{1}{2} \sigma_y d\sigma_y \dots \dots (6.34)$$

If during biaxial loading the ratio of $d\sigma_x$ and $d\sigma_y$ is taken according to equation (6.33), then integrating equation (6.34) gives

$$J_2 = J_2^* + \sigma_y^2 = \frac{1}{3} \sigma_x^{*2} + \sigma_y^2 \quad \dots \quad (6.35)$$

Applying equations (6.8) to (6.11) to the computation of the moduli D_x , D_y and D_{xy} as defined by equation (3.6) gives:

$$D_x = \frac{S}{RS - T^2} \quad \dots \quad (6.36)$$

$$D_y = \frac{R}{RS - T^2} \quad \dots \quad (6.37)$$

$$D_{xy} = D_{yx} = \frac{T}{RS - T^2} \quad \dots \quad (6.38)$$

where

$$R = \frac{1}{E} + \frac{4}{9} F \sigma_x^{*2} \quad \dots \quad (6.39)$$

$$S = \frac{1}{E} + \frac{1}{9} F \left(\frac{3}{2} \sigma_y - \sigma_x^* \right)^2 \quad \dots \quad (6.40)$$

$$T = \frac{\nu}{E} - \frac{2}{9} F \sigma_x^* \left(\frac{3}{2} \sigma_y - \sigma_x^* \right) \quad \dots \quad (6.41)$$

The results are shown graphically in Fig. 12 for $\sigma_x^* = 36$ ksi and $\sigma_x^* = 54$ ksi. From these results it can be concluded that the influence of the magnitude of σ_x^* is negligibly small. It is not obvious, however, which values of D_x , D_y and D_{xy} should be selected as being applicable in the strain-hardening range. Fortunately, compression tests on wide-flange sections presented in Chapter 7 reveal that the ratios of the half-wave

length of the buckled shape over the depth of the section for the cases of web buckling are 0.55 and 0.54 (Tests D4 and D6 respectively). According to equation (3.21) this ratio is equal to $\sqrt[4]{D_x/D_y}$ if the small restraining effects of the flanges are neglected. Figure 13 shows the influence of σ_y/σ_x^* on $\sqrt[4]{D_x/D_y}$. On account of the results of the web buckling tests the values of D_x , D_y and D_{xy} corresponding to $\sigma_y/\sigma_x^* = 0.34$ have been selected as applicable to the strain-hardening range.

Thus

$$\begin{aligned}D_x &= 3,000 \text{ ksi} \\D_y &= 32,800 \text{ ksi} \\D_{xy} &= D_{yx} = 8,100 \text{ ksi}\end{aligned}$$

7. COMPARISON WITH TEST RESULTS

For the selection of applicable values of D_x , D_y , D_{xy} , D_{yx} and G_t use has been made of the results of local (plate) buckling tests. The results are summarized here and are presented in more detail in another paper⁽¹⁹⁾.

7.1 Compression Tests on Angles

A number of compression tests on angles were performed with the purpose of checking the theoretical estimates developed above. Angle specimens have better known boundary conditions than WF sections and therefore give a more positive check. When buckling torsionally under the action of an axial load, the flanges of the angle act as two plates each with one free and one hinged edge, the heel forming the hinged edge. The loaded ends of the column were fixed against rotation in the testing machine. The dimensions of all specimens are given in Table 2. Besides the longitudinal strains at the flange tips and the heel, the rotation of the center section was measured. From the rotation measurements the critical average strain was determined. The results of the angle tests are summarized in Table 3.

When all of the material is strained into the strain-hardening range ($\epsilon_{cr} \geq \epsilon_0$) the theoretical solution is given by equation (3.12), the length of the angle specimen being $2L$. A solution for the yielding range ($\epsilon_f < \epsilon_{cr} < \epsilon_0$) can be derived if the following three assumptions are made:

1. The material is elastic up to the yield stress.
2. In the yield range the specimen is partly elastic and partly strain-hardened.
3. The strain-hardening zones initiate at both ends and move toward the middle.

From the first assumption it follows that, if $\sigma_{cr} \leq \sigma_0$ the critical stress is given by

$$\sigma_{cr} = \left(\frac{t}{b}\right)^2 \left[\frac{\pi^2 E}{12(1-\nu^2)} \left(\frac{b}{L}\right)^2 + G \right] \quad \dots \quad (7.1)$$

When σ_{cr} obtained from equation (7.1) exceeds σ_0 yielding will have commenced. From the second assumption it then follows that the middle section, being still elastic, is practically rigid compared with the yielded zones. Assuming that only the latter will deform results in the following expression for the buckling stress

$$\sigma_{cr} = \sigma_0 = \left(\frac{t}{b}\right)^2 \left[\frac{\pi^2 D_x}{12} \left(\frac{b}{\xi L}\right)^2 + G_t \right] \quad \dots \quad (7.2)$$

where

$$\xi L = \text{length of each yielded zone}$$

The corresponding critical strain is

$$\epsilon_{cr} = (1 - \xi) \epsilon_f + \xi \epsilon_0 \quad \dots \quad (7.3)$$

Substituting in equation (7.2) the values of D_x and G_t this equation determines the relationship between b/t and ξ . For $L/b = 2.65$, the average value of the tested sections, the b/t vs ξ curve has been plotted in Fig. 14 as a solid line. As elastic deformations have been neglected in equation (7.2) $b/t = \infty$ for $\xi = 0$. For this case $b/t = 20.7$ which is found from equation (7.1) by taking $\sigma = 36$ ksi and $L/b = 2.65$.

Knowing the rigid plastic solution and the point for $\xi = 0$ of the elastic-plastic solution the latter has been sketched in Fig. 14 as a dotted line. The elastic-plastic solution of b/t vs ξ with equation (7.3) gives ϵ_{cr} as a function of b/t for the range $\epsilon_f < \epsilon_{cr} < \epsilon_0$. The complete theoretical

205E.7

curves are shown in Fig. 15 for $L/b = \infty$ and $L/b = 2.65$, and are compared with the test results. The theoretical curves give a good description of the buckling strength.

7.2 Tests on Wide-Flange Shapes

In order to investigate the actual behavior of WF shapes with regard to local buckling, six different shapes were each tested under two loading conditions:

- (a) Axial compression (Test D1, D2, D3, D4, D5, D6)
- (b) Pure Bending (Test B1, B2, B3, B4, B5, B6)

The dimensions of all WF specimens are given in Table 4 and the test results are summarized in Table 5.

For the cases where flange buckling was predominant the critical strains of the flanges vs the b/t ratios and the theoretical curves are plotted in Fig. 16. The theoretical solution is given by equation (3.10). The results of tests D4 and D6 are omitted because web buckling occurred first and obviously caused premature flange buckling. Furthermore specimen B4 did not develop a major flange buckle but failed by lateral buckling. Therefore this result has also been eliminated from Fig. 16. From this figure it can be concluded that, if premature web buckling is prevented, the webs of the tested sections provide some restraint to the flanges corresponding to a value of β from 0 to about 0.05. Comparing the theoretical values of the half-wave length over flange width ratio given by equation (3.11) and plotted in Fig. 17, with the measured values of the bending tests given in Table 5 shows that the theory gives a good description of the actual behavior. For the axial loading tests the half-wave length was obviously influenced by web buckling, except for specimen D5 which had the smallest d/t ratio.

For the cases where web buckling occurred first (Test D4 and D6) or simultaneous with flange buckling (Test D2) the critical strains are plotted vs the d/t ratios as in Fig. 18. Comparison is made with the theoretical solutions given by equations (3.20) and (3.22) for the cases of zero and full restraint respectively. Again favorable agreement is obtained. The values of l/d given by equation (3.21) and plotted in Fig. 19 necessarily agree with the experimental values because D_x and D_y were selected in view of these test results.

7.3 Summary

The results of the investigation presented in this paper can be divided into two parts: firstly the derivation of stress-strain relations for the strain-hardening range of structural steel and secondly their application to the plate buckling problem.

Effective stress-strain relations were determined describing the orthotropic behavior of steel after it has been compressed into the strain-hardening range. The following values of the moduli were found to be applicable:

$$\begin{aligned} D_x &= 3,000 \text{ ksi} \\ D_y &= 32,800 \text{ ksi} \\ D_{xy} &= D_{yx} = 8,100 \text{ ksi} \\ G_t &= 2,400 \text{ ksi} \end{aligned}$$

It is considered that the agreement between theory and test results (Figs. 15, 16, and 18) justifies this approach to the problem.

A direct practical application of the findings presented in this paper is the prevention of local buckling of outstanding flanges in continuous frames, in which the design is based upon ultimate strength.

From the required rotation capacity of the plastic hinges the strains of the flanges can be determined. Fig. 16 then gives the required b/t ratio, for $\beta = 0.01$.

These stress-strain relations could equally well be applied to other problems involving the occurrence of shear and biaxial stresses and strains in the strain-hardening range of steel.

8. A C K N O W L E D G M E N T S

This paper is based on a Ph.D. dissertation presented to the Graduate Faculty of Lehigh University. The author is greatly indebted to Dr. Bruno Thürlimann who supervised the research project. His advice and suggestions are sincerely appreciated.

The project was part of the research program "Welded Continuous Frames and Their Components", carried out at Fritz Engineering Laboratory, Lehigh University, Bethlehem, Pennsylvania under the general direction of Dr. Lynn S. Beedle; the investigation is sponsored jointly by the Welding Research Council and the Department of the Navy with funds furnished by the American Institute of Steel Construction, American Iron and Steel Institute, Column Research Council (Advisory), Office of Naval Research (Contract 39303), Bureau of Ships and Bureau of Yards and Docks. Professor William J. Eney is Director of Fritz Engineering Laboratory and Head of the Department of Civil Engineering.

9 REFERENCES

1. Timoshenko, S., "THEORY OF ELASTIC STABILITY", McGraw-Hill, New York, 1936.
2. Bleich, F., "BUCKLING STRENGTH OF METAL STRUCTURES", McGraw-Hill, New York, 1952.
3. Nadai, A., "THEORY OF FLOW AND FRACTURE OF SOLIDS", McGraw-Hill, New York, 1950.
4. Bijlaard, P. P., "SOME CONTRIBUTIONS TO THE THEORY OF ELASTIC AND PLASTIC STABILITY", International Association for Bridge and Structural Engineering, Vol. VIII, 1947.
5. Ilyushin, A. A., "STABILITY OF PLATES AND SHELLS BEYOND THE PROPORTIONAL LIMIT", (Translated from Russian), NACA TM-116, October, 1947.
6. Stowell, E. Z., "A UNIFIED THEORY OF PLASTIC BUCKLING OF COLUMNS AND PLATES", NACA Report 898, 1948.
7. Handelman, G. H. and Prager, W., "PLASTIC BUCKLING OF A RECTANGULAR PLATE UNDER EDGE THRUSTS", NACA TN-1530, August, 1948.
8. Drucker, D. C., "STRESS-STRAIN RELATIONS IN THE PLASTIC RANGE -- A SURVEY OF THEORY AND EXPERIMENT", Report All S1, Graduate Division of Applied Mathematics, Brown University, December, 1950.
9. Onat, E. T. and Drucker, D. C., "INELASTIC INSTABILITY AND INCREMENTAL THEORIES OF PLASTICITY", Journal of the Aeronautical Sciences, Vol. 20, No. 3, March, 1953.
10. Haaijer, G. and Thurlimann, B., "COMBINED COMPRESSION AND TORSION OF STEEL TUBES IN THE STRAIN-HARDENING RANGE", Fritz Laboratory Report 241.2, Lehigh University (in preparation).
11. Girkmann, K. "FLACHENTRAGWERKE", 2nd Edition, Springer Verlag, Vienna, 1948.
12. Lundquist, E. E. and Stowell, E. Z., "CRITICAL COMPRESSIVE STRESS FOR OUTSTANDING FLANGES", NACA Report 734, 1942.
13. Lundquist, E. E. and Stowell, E. Z., "CRITICAL COMPRESSIVE STRESS FOR FLAT RECTANGULAR PLATES SUPPORTED ALONG ALL EDGES AND ELASTICALLY RESTRAINED AGAINST ROTATION ALONG THE UNLOADED EDGES", NACA Report No. 733, 1942.

14. Sokolnikoff, I. S., "MATHEMATICAL THEORY OF ELASTICITY", McGraw-Hill, New York, 1946.
15. Prager, W., "RECENT DEVELOPMENTS IN THE MATHEMATICAL THEORY OF PLASTICITY", Journal of Applied Physics, Vol. 20, Nr 3, 1949.
16. Wilder, T. W., III; Brooks, W. A., Jr.; and Mathauser, E. E., "THE EFFECT OF INITIAL CURVATURE ON THE STRENGTH OF AN INELASTIC COLUMN", NACA TN 2872, January, 1953.
17. Huber, A. W. and Beedle, L. S., "RESIDUAL STRESS AND THE COMPRESSIVE STRENGTH OF STEEL", Welding Journal, 33 (12), December, 1954.
18. Ramberg, W. and Osgood, R., "DESCRIPTION OF STRESS-STRAIN CURVES BY THREE PARAMETERS", NACA TN 902, 1943.
19. Haaijer, G. and Thürlimann, B., "ON INELASTIC LOCAL BUCKLING IN STEEL", A Theoretical and Experimental Study with Recommendations for the Geometry of Wide-Flange Shapes in Plastic Design, Fritz Laboratory Report 205E.8, Lehigh University, August, 1956.
20. Haaijer, G. "LOCAL BUCKLING OF WIDE FLANGE SHAPES", Ph.D. Dissertation 1956, Lehigh University.

10. NOMENCLATURETensor Notation

- F = function defined by equation (4.1)
 f = yield and loading function
 i, j, k, l, m - are letter subscripts taking the values 1, 2, and 3
 J_2 = second invariant of deviatoric stress tensor
 k = constant
 s = mean normal stress
 s_{ij} = components of deviatoric stress tensor
 x_i = coordinate axis
 δ_{ij} = Kronecker delta
 ϵ_{ij} = components of strain tensor
 ϵ_{ij}^e = elastic strain component
 ϵ_{ij}^p = plastic strain component
 σ_{ij} = components of stress tensor

Engineering Notation

- A, a_1, a_2 - are constants
 B = constant
 b = width of plate with one free edge
 $C_1, C_2, C_3, C_4, C_5, C_6, C_7$ - are constants
 $D_x = \frac{E_x}{1 - \nu_x \nu_y}$
 $D_y = \frac{E_y}{1 - \nu_x \nu_y}$
 $D_{xy} = \nu_y D_x$
 $D_{yx} = \nu_x D_y$
 d = width of plate supported along all four edges

E	=	modulus of elasticity
E_t	=	tangent modulus
E_x	=	tangent modulus in x - direction
E_y	=	tangent modulus in y - direction
E_0	=	strain-hardening modulus
f	=	ratio of \bar{y} over depth of simplified column
f_0	=	value of f at initiation of strain-hardening
f_s	=	value of f at which strain reversal takes place
G	=	modulus of elasticity in shear
G_t	=	tangent modulus in shear
H	=	function defined by equation (3.6)
h	=	thickness of sheet forming simplified cruciform section
I	=	moment of inertia per unit width of plate
K	=	constant
K_x	=	curvature of plate in x - direction
K_y	=	curvature of plate in y - direction
K_{xy}	=	twist of plate
l	=	half-wave length of buckled shape
M_x	=	bending moment per unit width of plate in x - direction
M_y	=	bending moment per unit width of plate in y - direction
M_{xy}	=	torsional moment per unit width of plate in ...
N_x	=	axial force per unit width of plate in x - direction
N_y	=	axial force per unit width of plate in y - direction
m	=	exponent in equation (6.1)
n	=	ratio of modulus of elasticity over tangent modulus
n'	=	ratio defined by equation (5.6)
R	=	function defined by equation (6.39)
S	=	function defined by equation (6.40)

- T = function defined by equation (6.41)
 t = thickness of plate
 w = deflection of plate
 x = coordinate axis
 y = coordinate axis
 y = deflection of simplified column
 \bar{y} = maximum value of y
 z = coordinate axis
- β = B/A = coefficient of restraint
 γ_{xy} = angular strain in xy plane
 ϵ_{cr} = critical strain corresponding to σ_{cr}
 ϵ_f = yield strain
 ϵ_0 = strain at initiation of strain-hardening
 ϵ_x = normal strain in x - direction
 ϵ_x^* = value of ϵ_x at which biaxial loading starts
 ϵ_y = normal strain in y - direction
 ϵ_y^* = value of ϵ_y at which biaxial loading starts
 ζ = coefficient determining length of yielded zone
 θ = angle of twist per unit length
 ν = Poisson's ratio
 ν_x = coefficient of dilatation for stress increment in x - direction
 ν_y = coefficient of dilatation for stress increment in y - direction
 σ_{cr} = critical (buckling) stress
 σ_e = elastic buckling stress
 σ_0 = yield stress
 σ_s = value of σ at which strain reversal takes place
 σ_x = normal stress in x - direction

σ_x^* = value of σ_x at which biaxial loading starts

σ_y = normal stress in y - direction

τ_{xy} = shear stress

ψ = function defined by equation (6.10)

Ψ = edge moment per unit length to produce unit rotation of edge

TABLE 1

RESULTS OF COMPRESSION COUPON TESTS

Coupon	Fritz Lab. Number	Section	σ_o ksi	ϵ_o $\times 10^3$	E_o ksi	Note
1	220A-UF3	14WF30	39.7	13.0	730	All WF section coupons taken from flanges
2	220A-UF4	"	41.5	14.6	690	
3	220A-LF1	"	42.5	14.6	650	
4	220A-LF2	"	39.0	12.5	790	
5	220A-LF3	"	39.7	12.5	730	
6	220A-LF4	"	42.0	13.0	670	
7	220A-A	"	40.8	15.0	640	
8	220A-B	"	40.8	12.5	675	
9	220A-D	"	40.3	15.5	650	
10	220A-E	"	39.6	14.5	650	
11	220A-F	"	35.3	(6.0)	780	
12	220A-G	"	36.2	(6.5)	700	
13	220A-B2F3	8WF31	40.0	17.4	770	
14	220A-B2F6	"	38.8	11.5	810	
15	220A-B2F7	"	39.0	14.8	730	
16	205E-C14	10WF33	40.0	14.5	855	
17	205E-C15	"	37.0	13.8	805	
18	205E-C2	8WF40	38.4	12.8	1060	
19	205E-C9	L6.6.3/8	39.0	12.8	710	
20	205E-C12	"	37.6	14.3	906	
21	205E-C13	"	35.1	14.6	845	
Average Values*			39.2	13.9	755	

* Numbers in parentheses not used for determining average value.

TABLE 2

DIMENSIONS OF ANGLE SPECIMENS

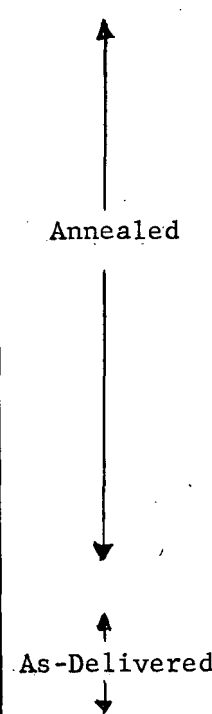
Specimen	Length 2L (in.)	Width b (in.)	Thickness t (in.)	b/t	2L/b	Material
A-21	25.0	4.87	0.383	12.70	5.14	 Annealed As-Delivered
A-22	25.0	4.79	0.381	12.60	5.21	
A-31	17.9	3.27	0.370	8.85	5.48	
A-32	17.9	3.28	0.374	8.79	5.46	
A-41	12.5	2.31	0.377	6.13	5.41	
A-42	12.5	2.34	0.371	6.36	5.35	
A-33	17.5	3.30	0.378	8.73	5.30	
A-51	21.2	4.07	0.380	10.70	5.21	

TABLE 3

RESULTS OF ANGLE TESTS

Test	σ_o ksi	$\epsilon_{cr} \cdot 10^3$	σ_{cr} ksi	Type of Buckling
A-22	--	3.0	32.2	torsional
A-31	34.9	16.5	35.8	torsional
A-32	34.6	16.5	35.6	torsional
A-41	35.3	--	--	bending
A-42	34.1	--	--	bending
A-33	41.3	16.0	46.4	torsional
A-51	41.0	6.0	41.2	torsional

TABLE 4

DIMENSIONS OF WF SPECIMENS

Spec.	Shape	2b in	t_f in	d in	t_w in	L in	L^1 in	b/t_f	d/t_w
B1 D1	10WF33	7.95	0.429	9.37	0.294	32	32	9.2	31.9
B2 D2	8WF24	6.55	0.383	7.63	0.236	26	26	8.6	32.3
B3 D3	10WF39	8.02	0.512	9.37	0.328	32	32	7.8	28.6
B4 D4	12WF50	8.18	0.620	11.57	0.351	32	32	6.6	33.0
B5 D5	8WF35	8.08	0.476	7.65	0.308	32	32	8.5	24.8
B6 D6	10WF21	5.77	0.318	9.56	0.232	23	26	9.1	40.9

2b = width of flange

t_f = thickness of flange

d = distance between center planes of flanges

t_w = thickness of web

L = length of compression specimen

L^1 = length of part of bending specimen subjected to pure bending

TABLE 5

RESULTS OF WF TESTS

Test	σ_o ksi	$\epsilon_{cr} \cdot 10^3$		σ_{cr} ksi		Flange l/b	Web l/d	Type of Buckling
		Flange	Web	Flange	Web			
D1	34.4	8.5	8.5	34.2	34.2	1.8	0.56	flange
D2	34.0	13.5	12.7	34.0	34.0	1.5	0.50	flange & web
D3	35.2	19.0	19.0	39.0	39.0	1.5	0.46	flange
D4	35.0	18.5	5.0	36.8	35.4	1.5	0.55	web
D5	36.6	17.0	17.0	38.0	38.0	2.1	0.56	flange
D6	38.0	4.3	1.6	33.8	37.2	--	0.54	web
B1	--	7.0	--	--	--	2.4	--	flange
B2	--	23.0	--	--	--	2.0	--	flange & lateral
B3	--	22.5	--	--	--	2.2	--	flange & lateral
B4	--	29.0	--	--	--	--	--	lateral
B5	--	22.0	--	--	--	2.0	--	flange & lateral
B6	--	14.0	--	--	--	2.4	--	flange & lateral

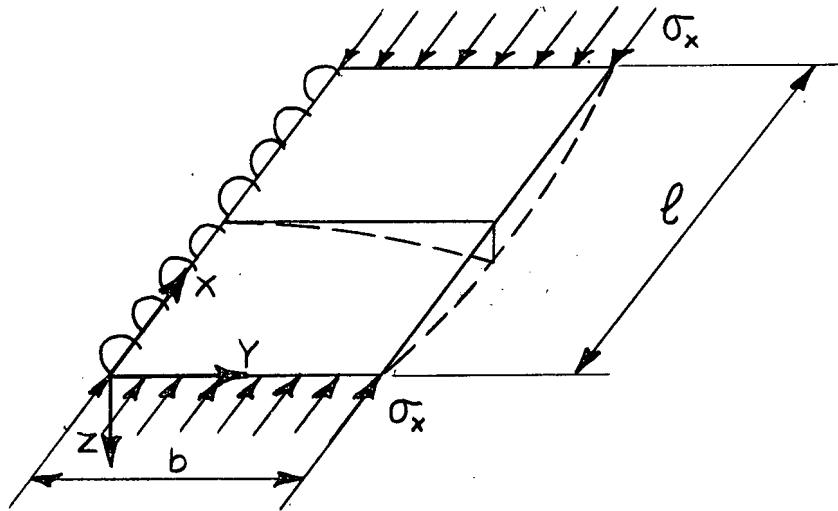


Fig. 1 - Plate with one free edge

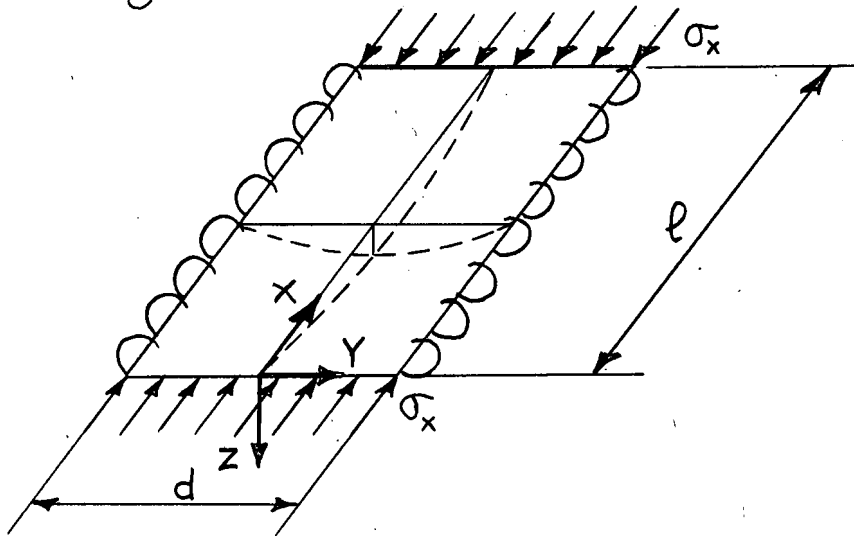


Fig. 2 - Plate supported at all four edges

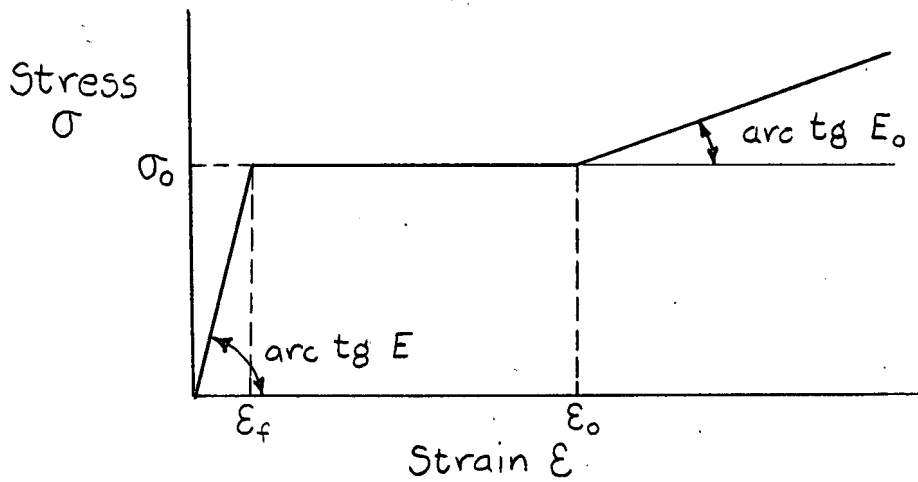


Fig. 3 - Simplified stress - strain curve

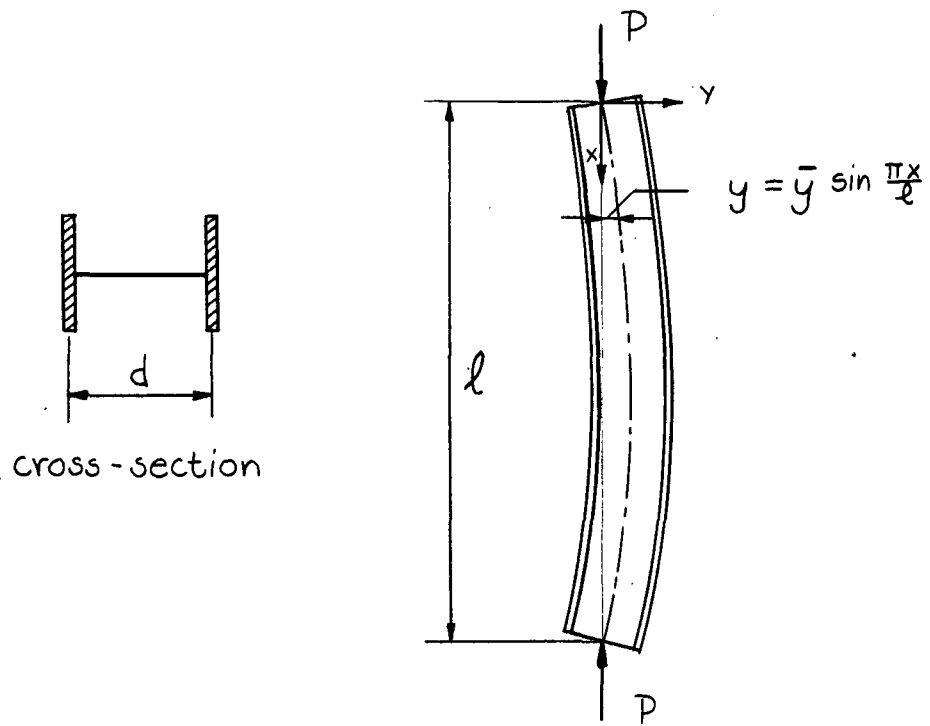


Fig. 4 - Simplified WF column

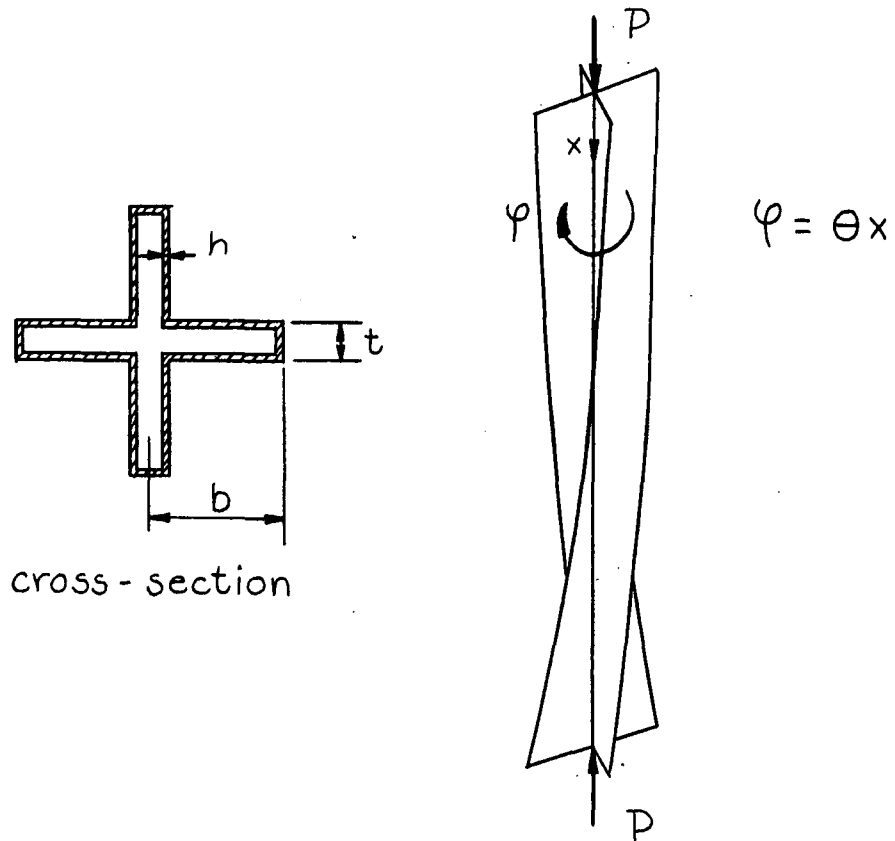


Fig. 5 - Simplified Cruciform Column

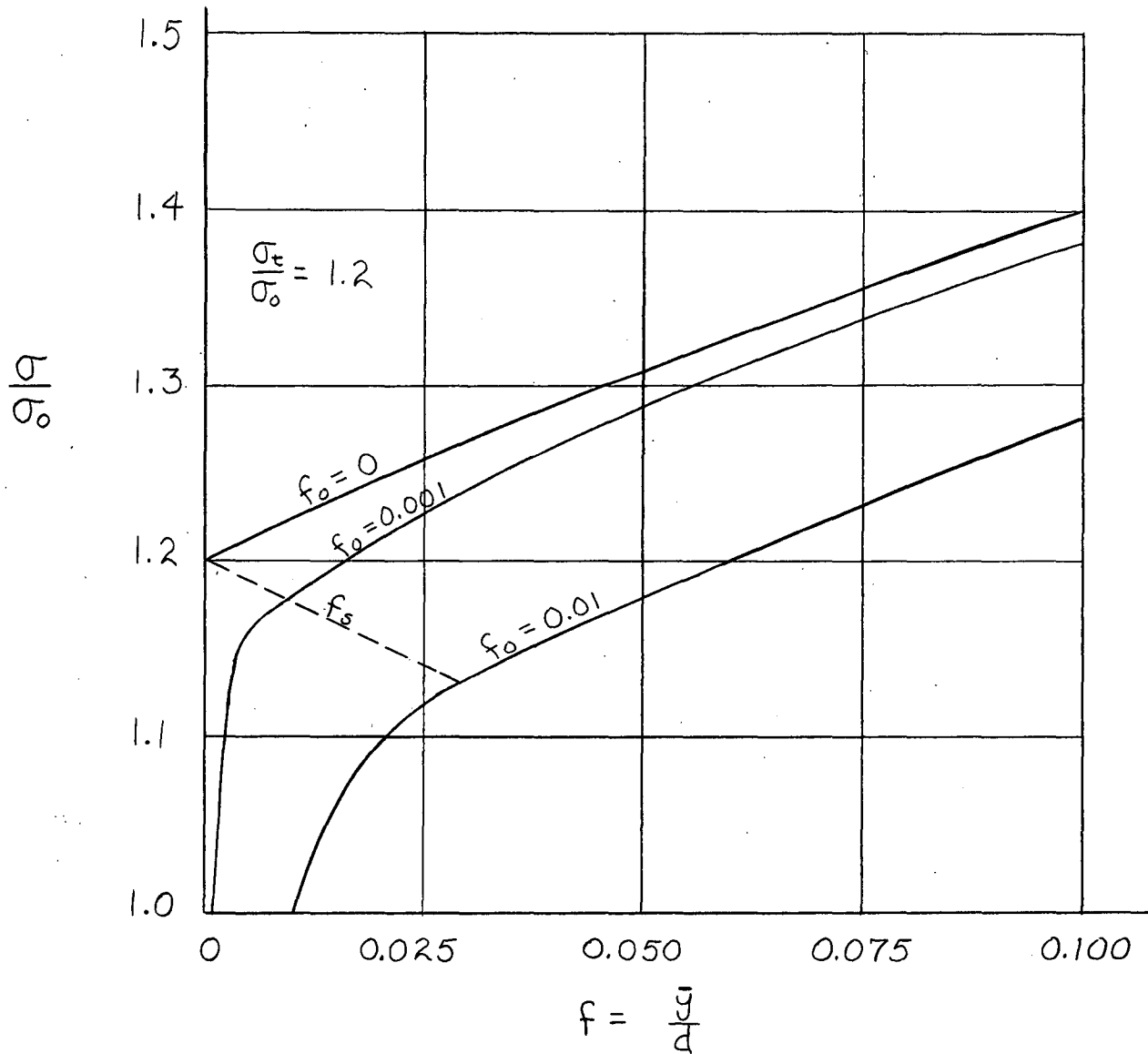


Fig. 6 - Effect of initial imperfections on a simplified WF section

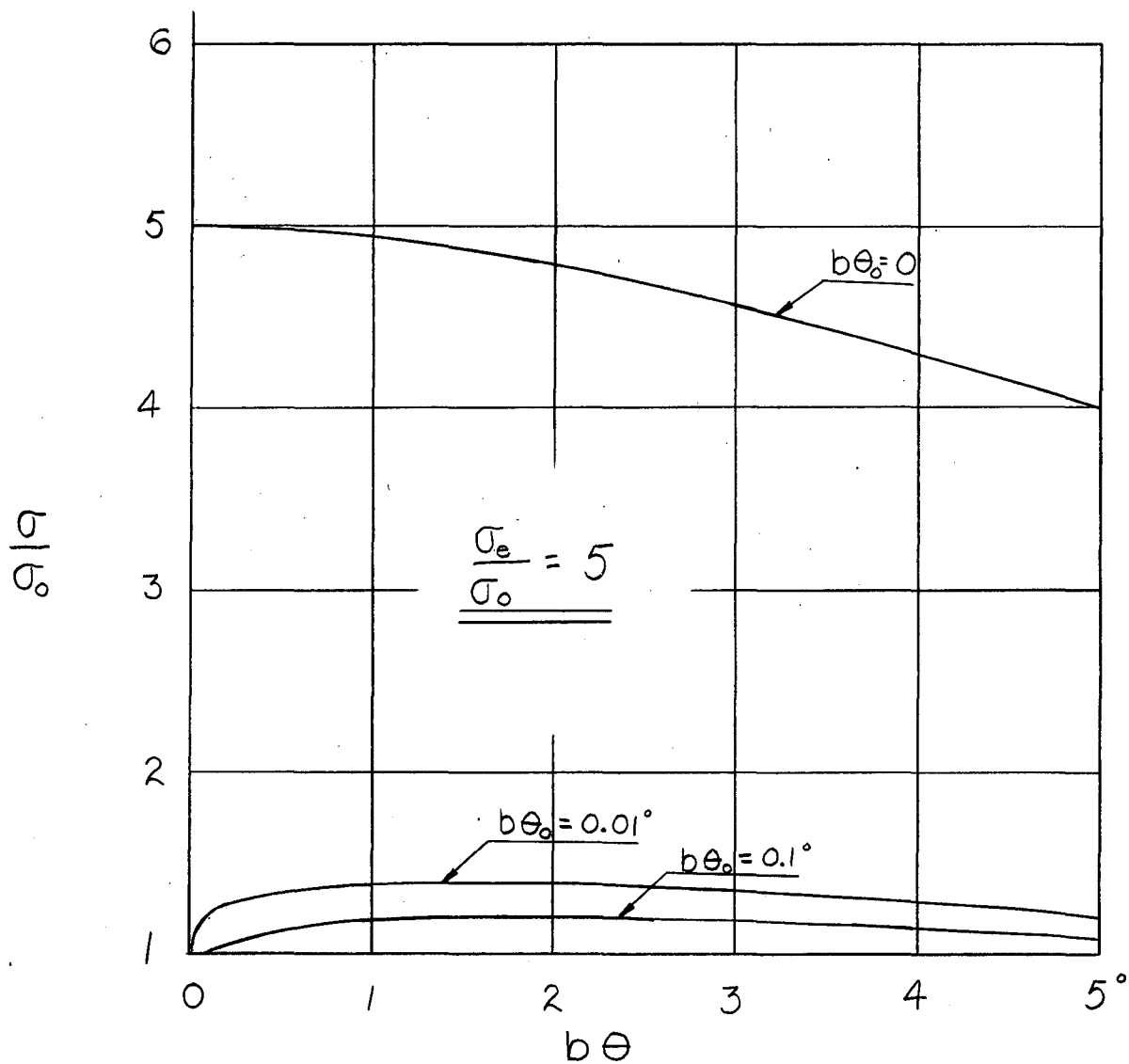


Fig. 7 - Influence of initial imperfections on a simplified cruciform section

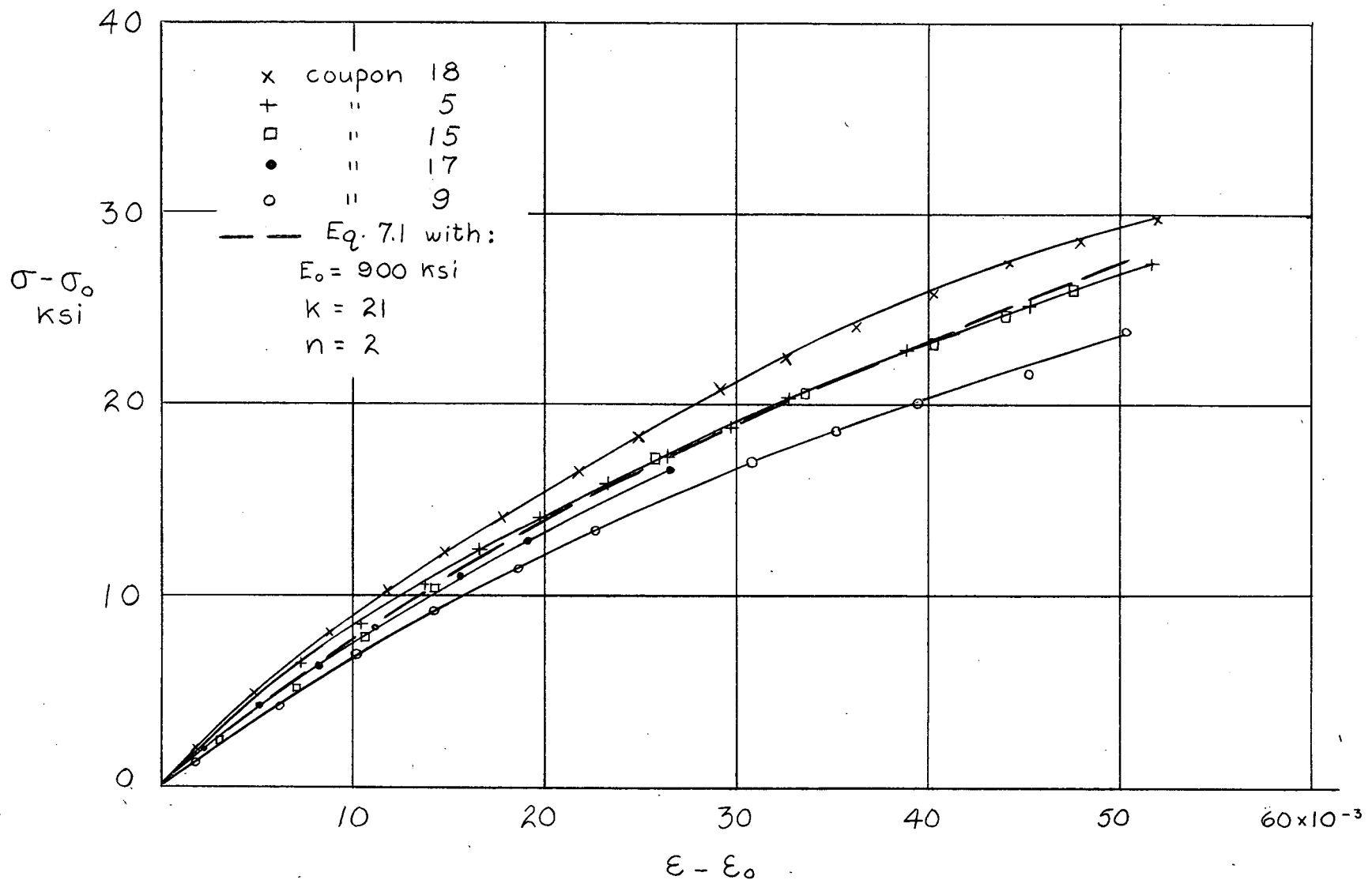


Fig. 8 - Results of Compression Coupon Tests in the Strain - Hardening Range

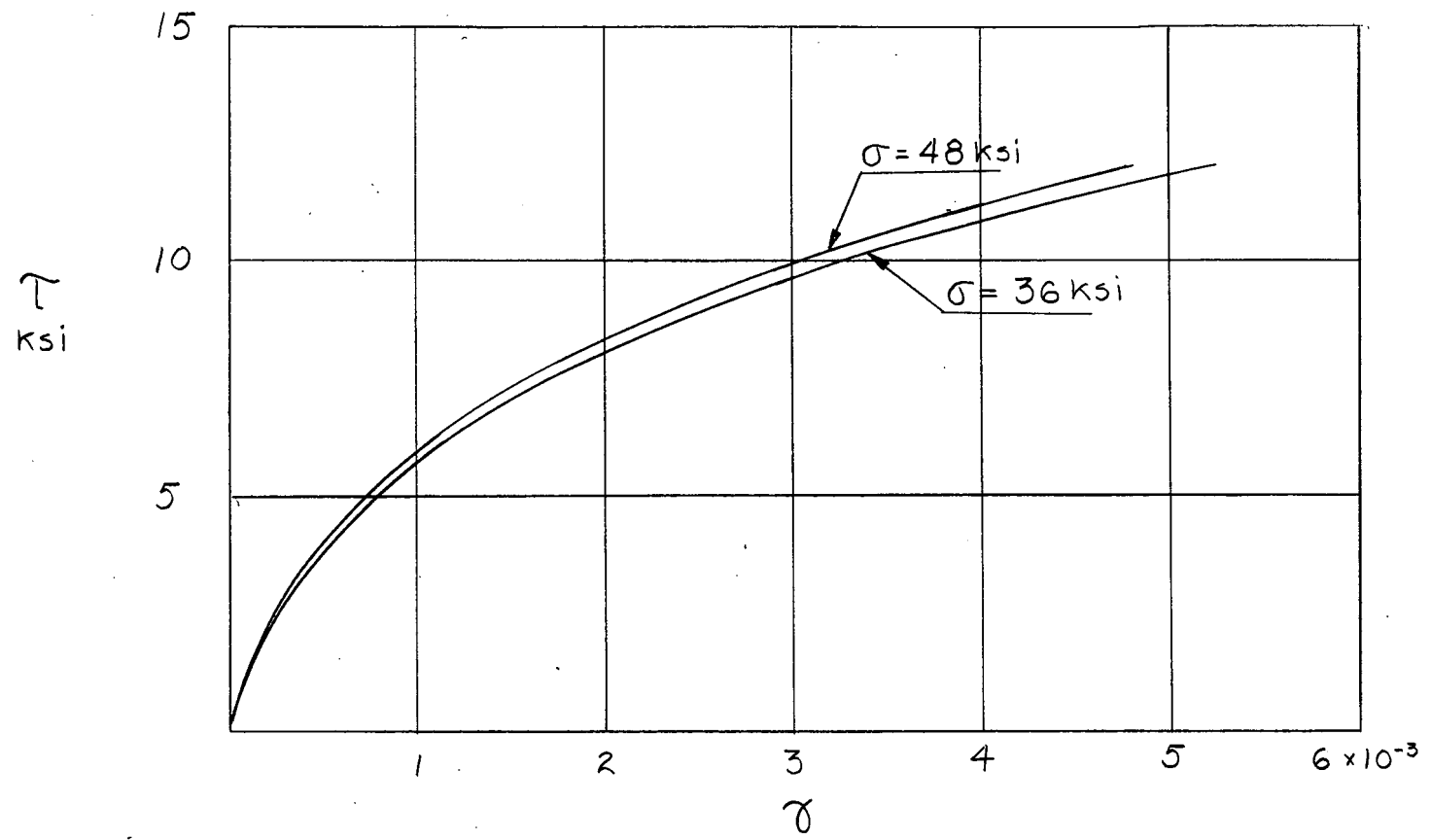


Fig. 9 - Superposition of Shear Stress on Constant Normal Stress

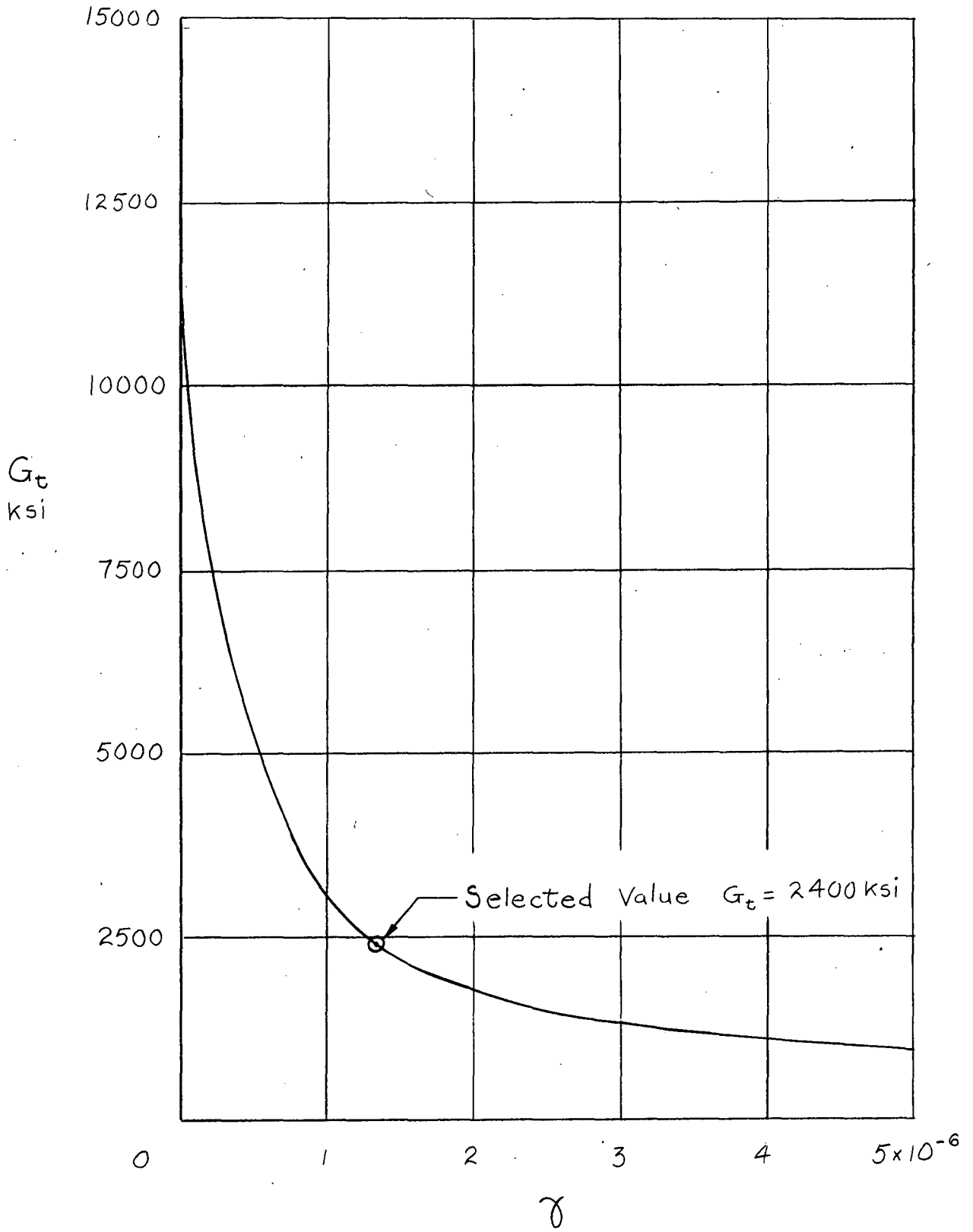


Fig. 10 - The Tangent Shear Modulus

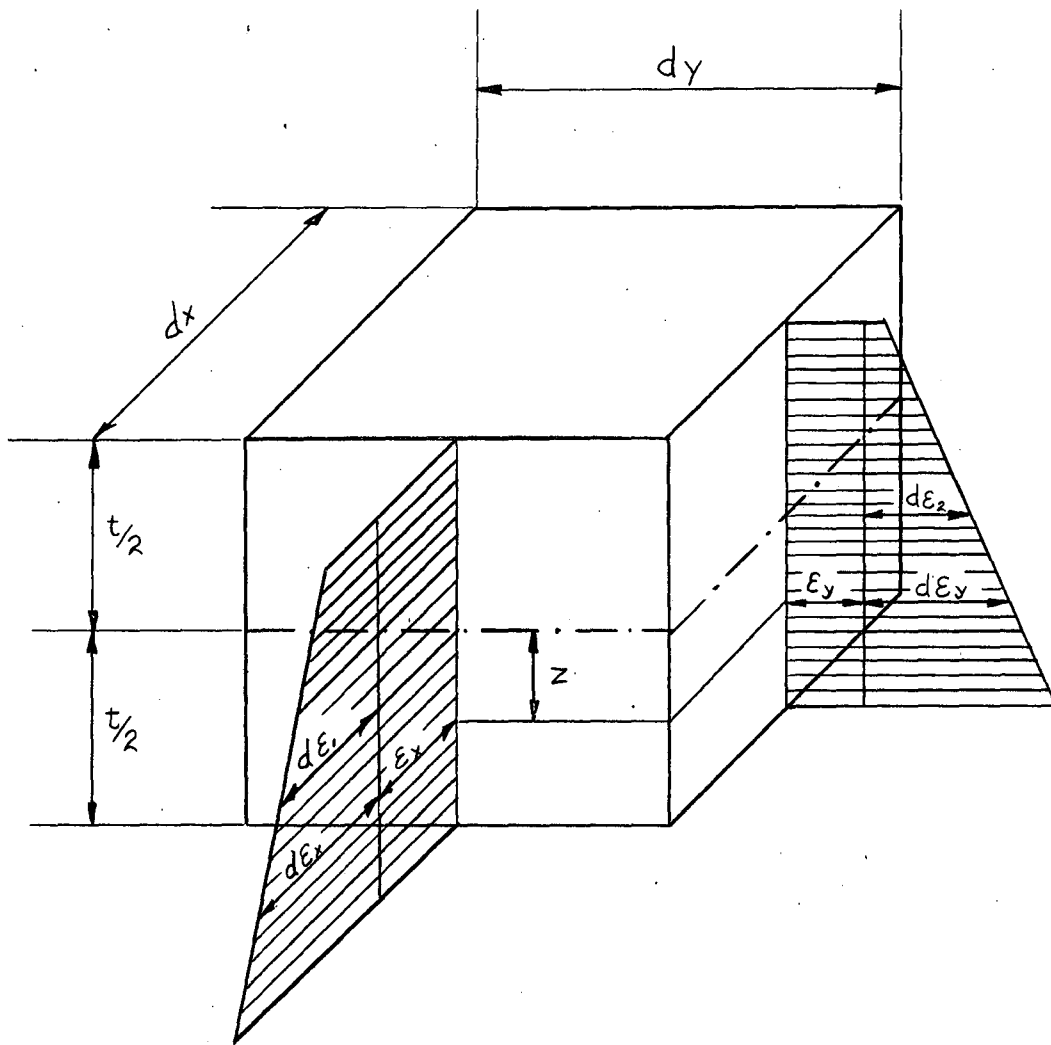


Fig. 11 - Assumed linear strain distribution

D_x
 D_y
 D_{xy}

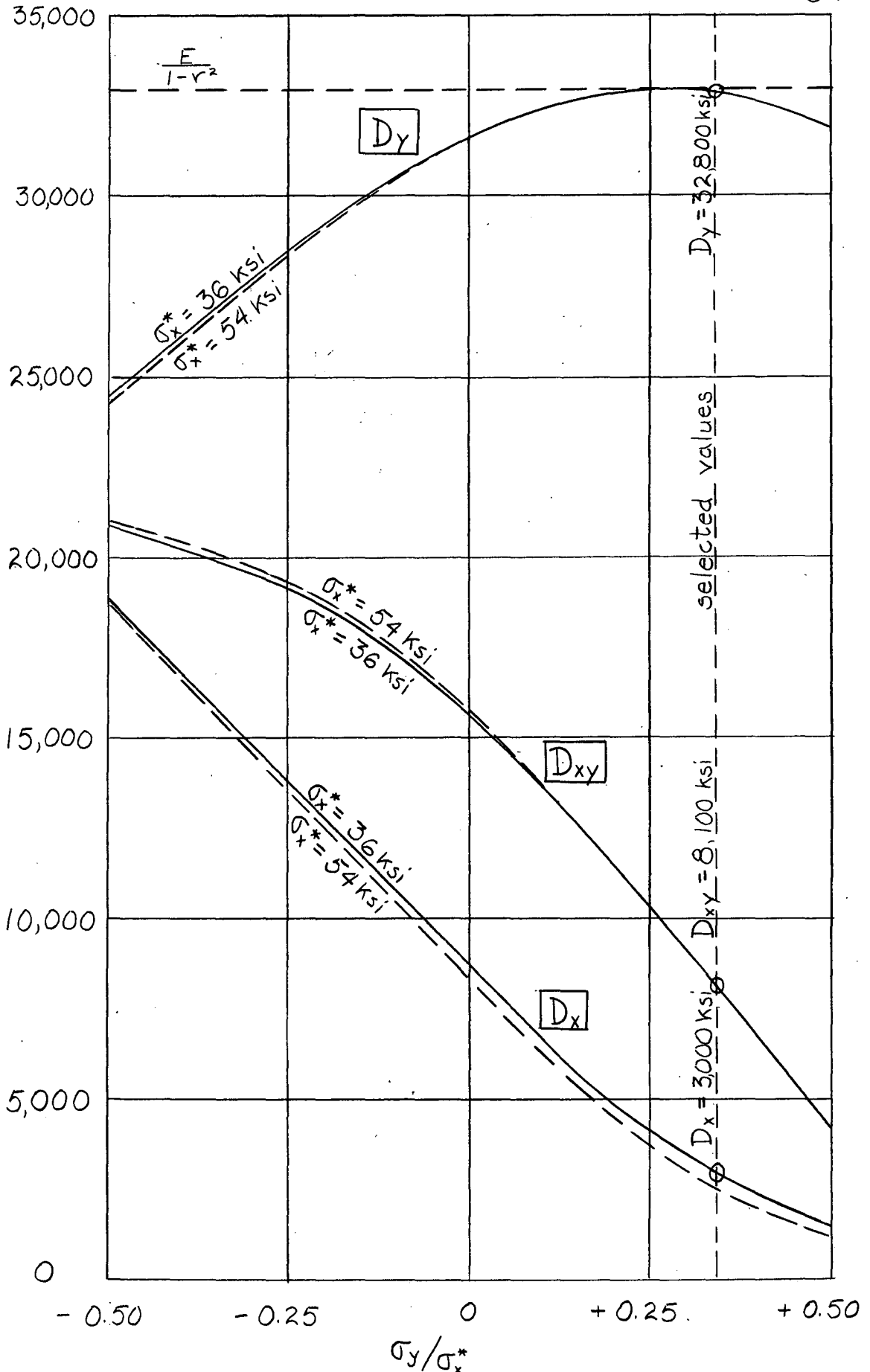


Fig. 12 - Influence of σ_y/σ_x^* on D_x , D_y , and D_{xy}

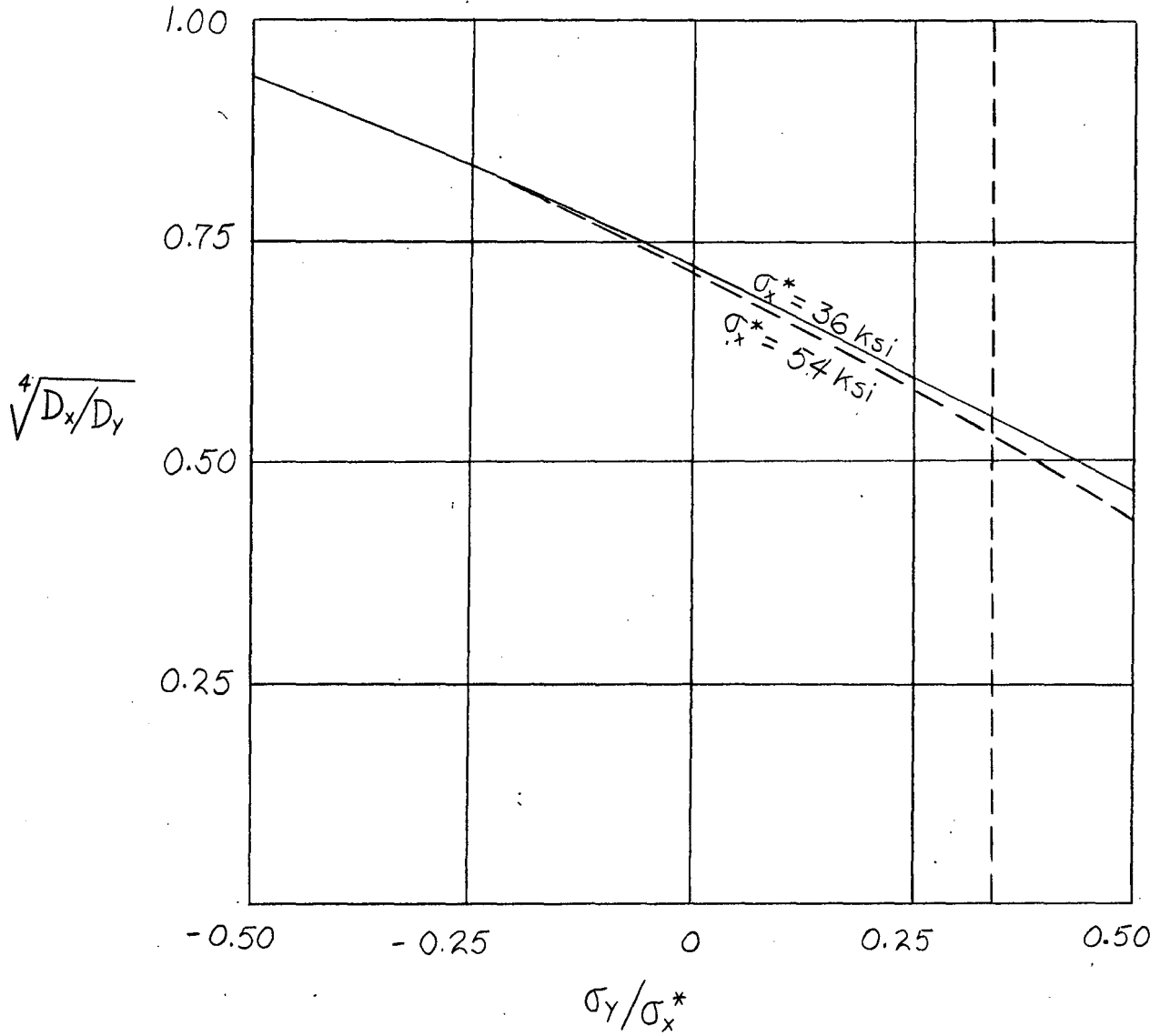


Fig. 13 - Influence of σ_y/σ_x^* on $\sqrt[4]{D_x/D_y}$.

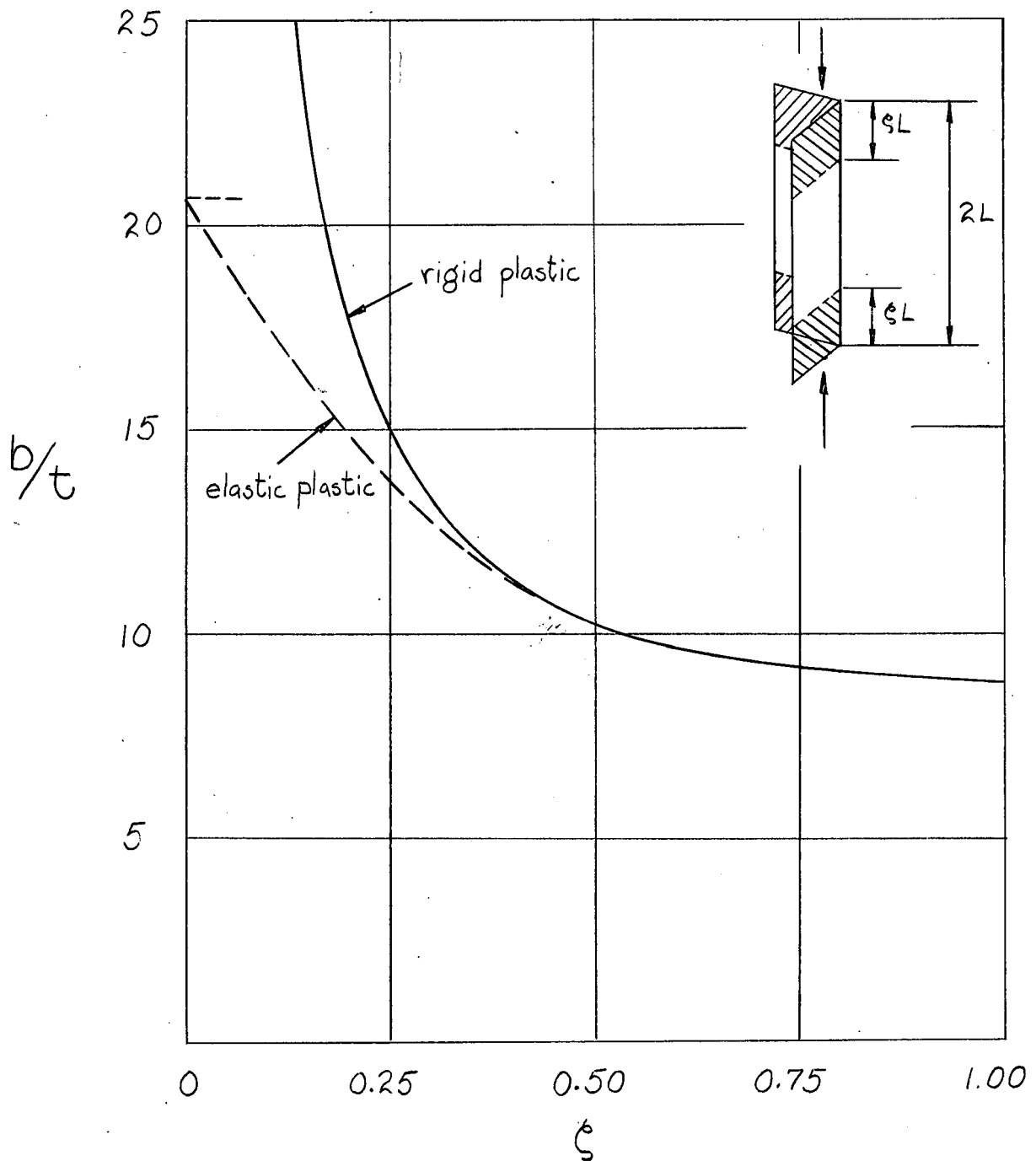


Fig. 14 - Yield Penetration ξ as a Function of b/t
for $L/b = 2.65$

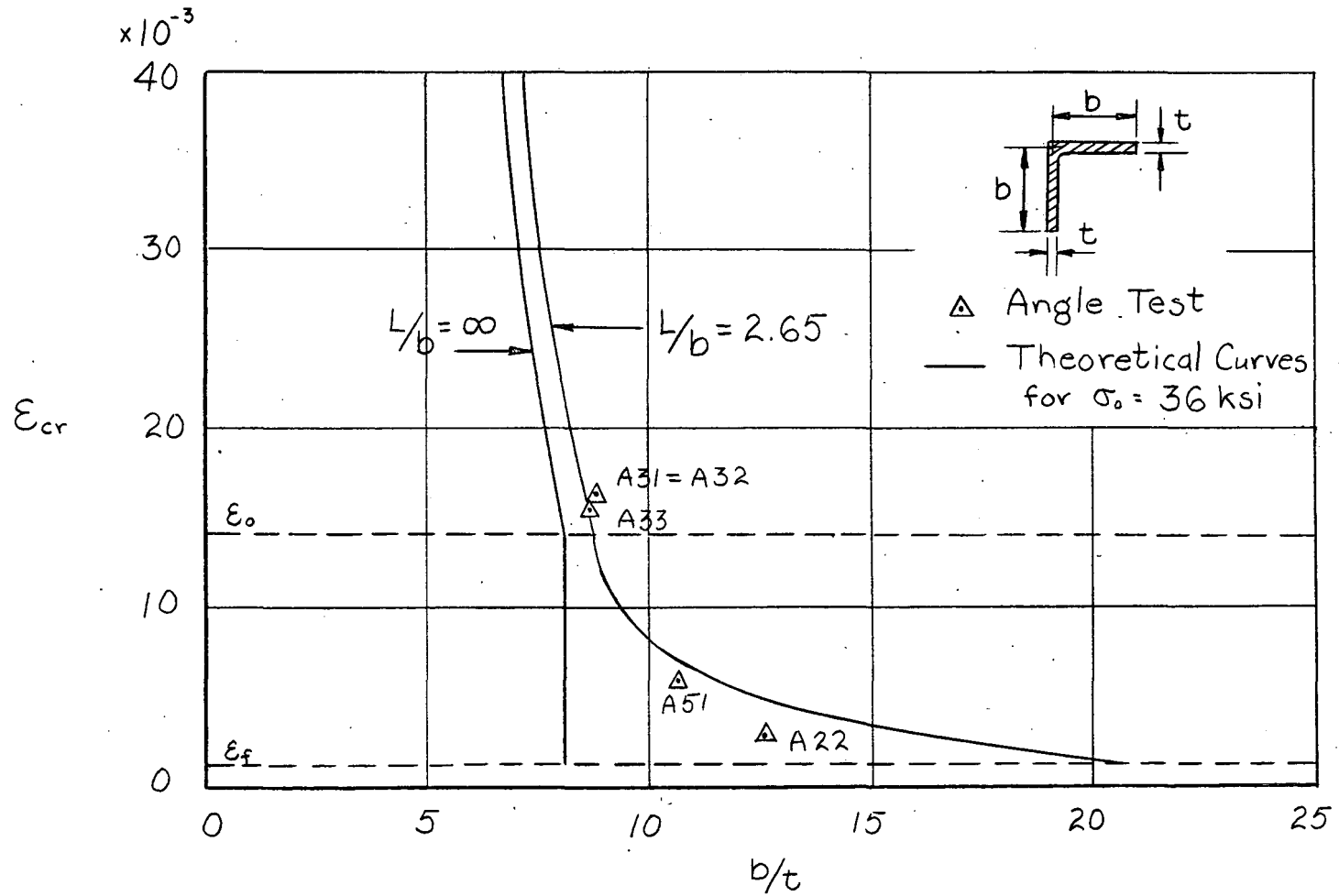


Fig. 15 - Comparison of Results of Torsional Buckling Tests on Angles with Theoretical Curves

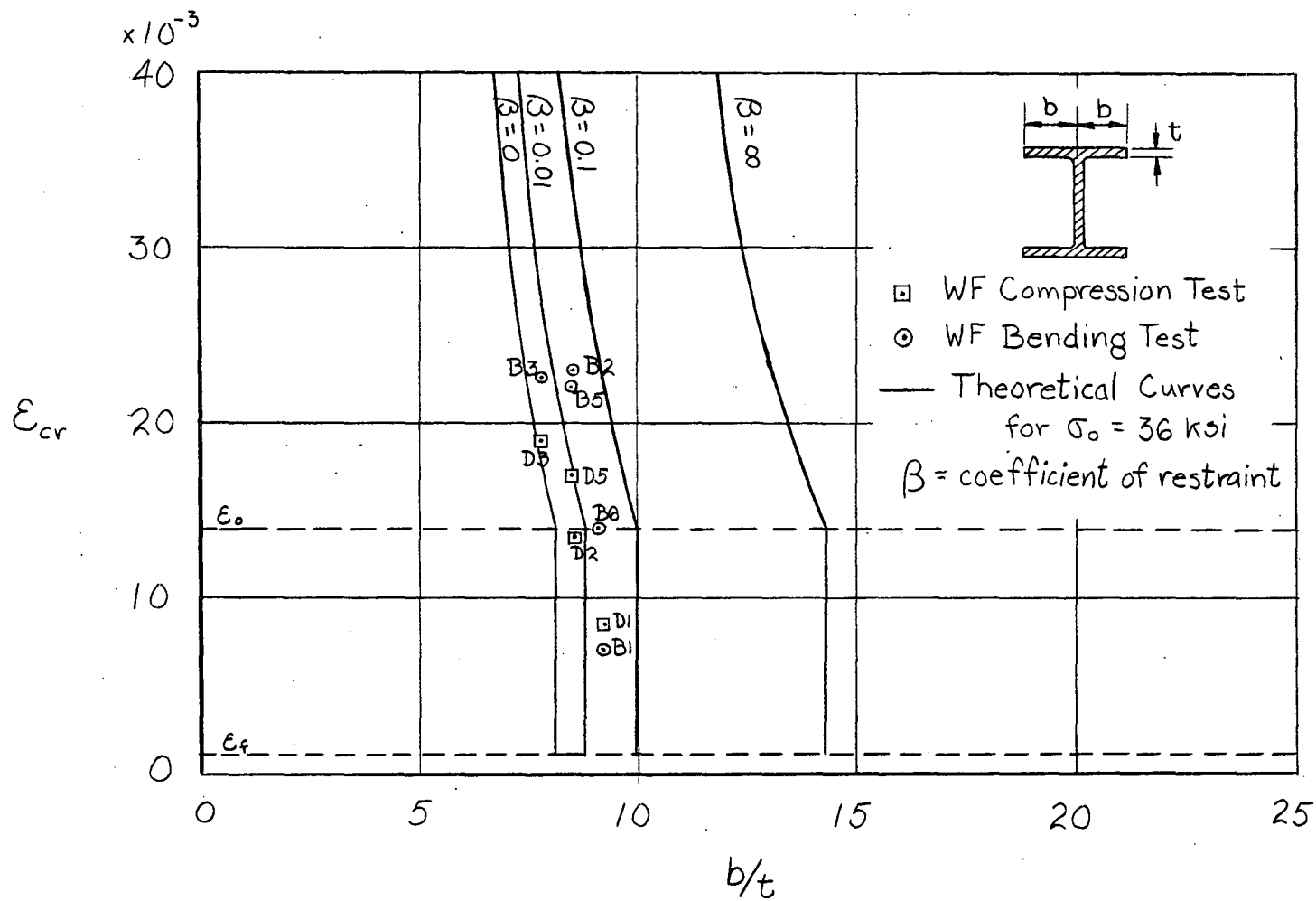


Fig. 16 - Buckling of Wide - Flange Shapes

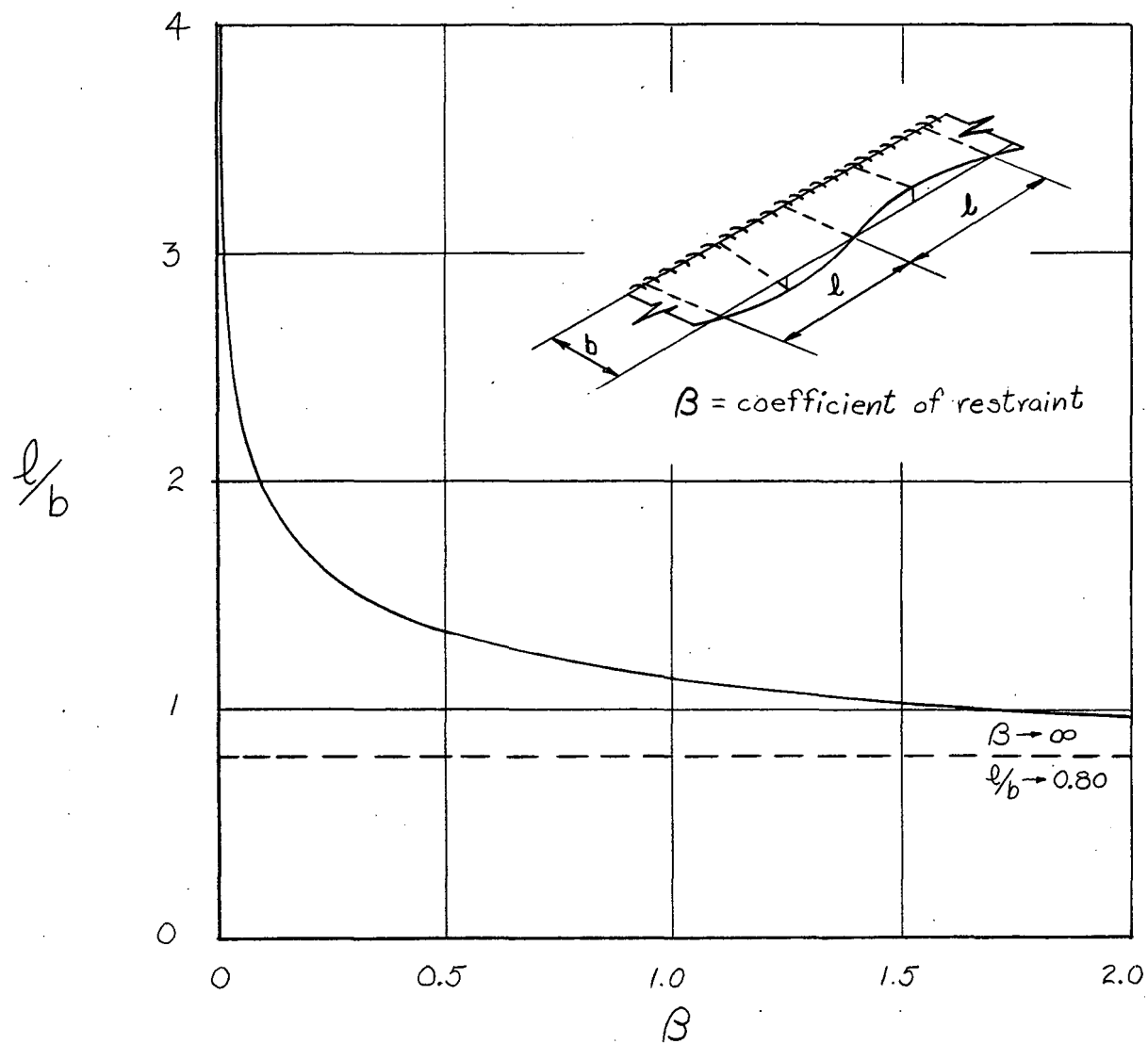


Fig. 17- Half-Wave Length of Outstanding Flanges

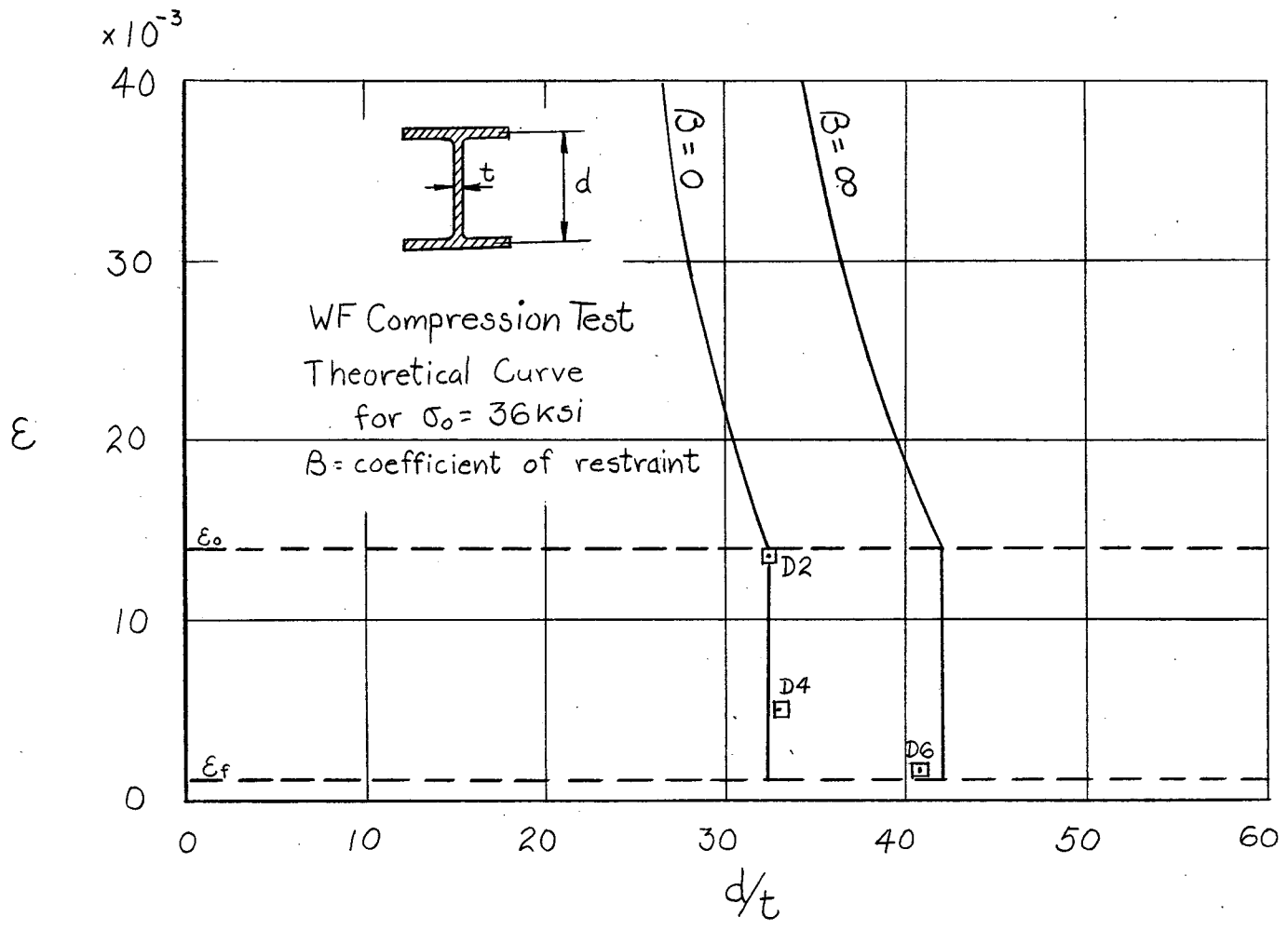


Fig. 18 - Buckling of Webs of Wide- Flanged Shapes (Uniform Compression)

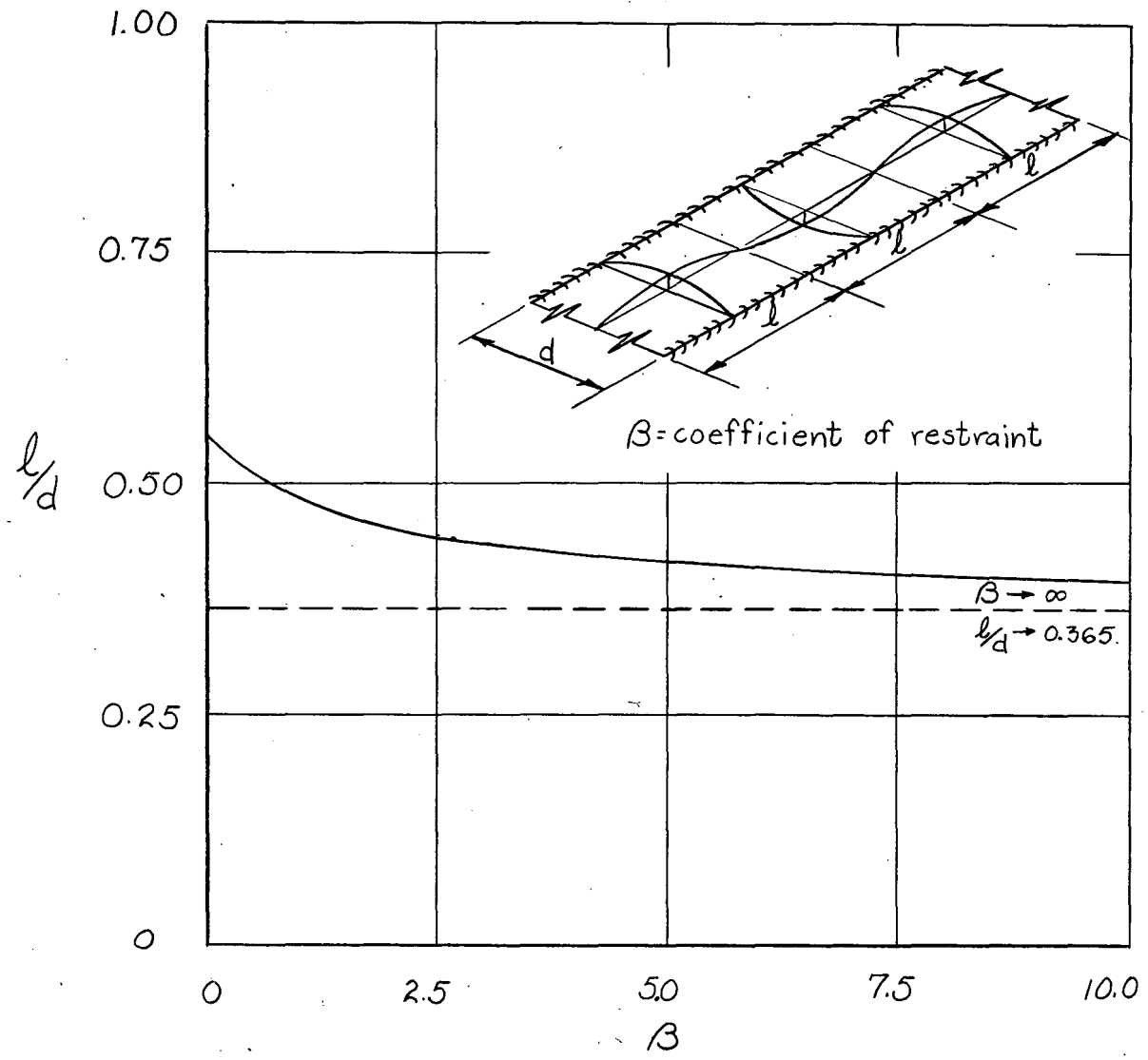


Fig. 19 - Half-wave length of webs